

COMPUTATIONALLY EFFICIENT ROBUST MODEL
PREDICTIVE CONTROL STRATEGIES FOR LINEAR
CONSTRAINED SYSTEMS

MARYAM BAGHERZADEH

A THESIS
IN
THE DEPARTMENT
OF
ELECTRICAL AND COMPUTER ENGINEERING

PRESENTED IN PARTIAL FULFILLMENT OF THE REQUIREMENTS
FOR THE DEGREE OF MASTER OF APPLIED SCIENCE
CONCORDIA UNIVERSITY
MONTRÉAL, QUÉBEC, CANADA

SEPTEMBER 2020

© MARYAM BAGHERZADEH, 2020

**CONCORDIA UNIVERSITY
SCHOOL OF GRADUATE STUDIES**

This is to certify that the thesis prepared

By: Maryam Bagherzadeh

Entitled: Computationally Efficient Robust Model Predictive Control Strategies for Linear Constrained Systems

and submitted in partial fulfillment of the requirements for the degree of

Master of Applied Science (Electrical and Computer Engineering)

complies with the regulations of this University and meets the accepted standards with respect to originality and quality.

Signed by the final examining committee:

_____	Chair
Dr. R. Selmic	
_____	External Examiner
Dr. Y. Zhang (MIAE)	
_____	Internal Examiner
Dr. R. Selmic	
_____	Supervisor
Dr. W. Lucia (CIISE)	

Approved by: _____
Dr. Y.R. Shayan, Chair
Department of Electrical and Computer Engineering

_____ 20____

Dr. Mourad Debbabi, Interim Dean,
Gina Cody School of Engineering and
Computer Science

Abstract

Computationally Efficient Robust Model Predictive Control Strategies for Linear Constrained Systems

Maryam Bagherzadeh

This thesis deals with control problem of designing low computationally demanding robust model predictive controllers (MPC) for constrained systems subject to states/input limitations and bounded disturbances. In particular, the proposed solutions are based on a dual-mode control paradigm known as Set-Theoretic MPC (ST-MPC). This control schemes are particularly appealing for their capability of reducing the typical computation burden of robust MPC controllers. The latter is obtained by moving most of the required computations into an off-line phase, while leaving a simple and real-time affordable computational algorithm in the on-line phase. In this work, such a paradigm has been properly extended to deal with regulation and tracking problems appearing in two different control applications, namely transient stability regulation in smart grid and reference tracking in multi autonomous vehicles.

In the transient stability control problem, we consider an operative scenario where a physical fault or a cyber-attack produces an impulsive state perturbation, and a controller must be designed to robustly recover, in a finite-time, transient stability despite initial perturbation and uncertainties. In such scenario, first we have used the standard feedback linearization technicalities to linearize the smart grid model, then, we have applied a set-theoretic MPC scheme to robustly regulate the state trajectory towards the transient stability region. Moreover, to validate the proposed theory, a simulation campaign has been performed to contrast the proposed solution with a state-of-the-art competitor. Simulation results has shown that the proposed strategy outperforms the competitor scheme both in terms of settling time and robustness.

In the multi-vehicle control problem, we exploit set-theoretic arguments to solve the reference tracking problem when the vehicles have different dynamics and/or constraints and/or disturbance, and each vehicle must follow uncoordinated reference trajectories. More in specific, we propose a novel control architecture where robust collision-free reference tracking is ensured by jointly using the set-theoretic control scheme and graph theory. To better clarify the potential and effectiveness of the proposed architecture, a simulation example involving 5 heterogeneous vehicles has been conducted.

Acknowledgments

I wish to express my sincere appreciation to my supervisor Dr. Walter Lucia who has the substance of a genius: he convincingly guided and encouraged me to be professional and move in the right direction even when the road got tough. The goal of this thesis would not have been realized without his continuous support and insightful comments. I am grateful to have had such a knowledgeable, considerate and outstanding supervisor.

Nobody has been more important to me in the pursuit of this thesis than the members of my family. I must express my very profound gratitude to my family whose love and guidance are with me in whatever I pursue. They are ultimate role models. This accomplishment would have not been possible without them.

Thank you to all my fellow lab-mates at Concordia University specially Kian, Mohsen, Shima and Amirreza for their help to color my life and the fun time we have had together.

Last but not least, thank you to my friends Reyhaneh, Nilou, Niki and Atefeh for providing me with unfailing support and continuous encouragement throughout my years of study.

Contents

List of Figures	viii
List of Tables	x
List of Abbreviations	1
1 Introduction	1
1.1 Literature review and motivation	1
1.1.1 Transient Stability Control Problem	4
1.1.2 Reference tracking in Multi Unmanned Vehicle systems	6
1.2 Thesis Contribution	8
1.3 Thesis Layout	9
1.4 Publications	10
2 Background on Set-Theoretic MPC	11
2.1 Preliminaries and Definitions	11
2.2 Set-Theoretic Model Predictive Control (ST-MPC)	13
2.2.1 Properties	15
2.3 ST-MPC Computation Algorithms	16
3 A Set-Theoretic Model Predictive Control Approach for Transient Sta-	
 bility in Smart Grid	18
3.1 Problem Formulation	18
3.2 Proposed Controller	24
3.2.1 Controller for Partial Coupling Compensation (u_i^f)	25

3.2.2	Set-theoretic controller for Robust Transient Stability (u_i^c)	25
3.2.3	Computational Algorithm and Controller Properties	29
3.3	Simulation	32
3.4	Conclusion	35
4	Guaranteed Collision Free Reference Tracking in Constrained Multi Vehicle Systems	39
4.1	Preliminaries and definitions	39
4.2	Problem Formulation	40
4.3	Proposed Solution	42
4.3.1	Set-Theoretic MPC Tracking Controller	43
4.3.2	Traffic Manager (TM) and Collision Avoidance	48
4.3.3	Computation Algorithms	52
4.4	Simulation	55
4.5	Conclusion	61
5	Conclusion	63
	Bibliography	65

List of Figures

1.1.1 Basic structure of Model Predictive Control	2
1.1.2 A discrete MPC scheme	2
2.2.1 N-step controllable family set	14
3.1.1 <i>New England 10 generator 39 bus power system</i>	19
3.1.2 <i>Generator i :Transient Stability Region.</i>	21
3.2.1 <i>Transient stability region Ξ_i^{ts} (blue rectangular region), RCI terminal region \mathcal{T}_i^0 (purple polyhedron), Family of robust one-step controllable sets $\{\mathcal{T}_i^j\}_{j=1}^N$ (blue polyhedra). Moreover, $x_i(0)$ is the initial perturbation and the black arrows show the state trajectory obtained from the proposed controller.</i> . . .	26
3.3.1 <i>i-th generator state trajectory $x_i(t)$ for $x_i(0) = [-50, 15]$</i>	36
3.3.2 <i>Rotor angle $\delta_i(t)$, Rotor angular speed $\omega_i(t)$ and Command Input $u_i^c(t)$: ST-MPC vs [34].</i>	36
3.3.3 <i>ST-MPC Domain of Attraction (DoA) and i-th generator state trajectories $x_i(t)$ for 10 different initial perturbations on the border of the DoA.</i>	37
3.3.4 <i>Rotor angular speed $\omega_i(t)$: ST-MPC vs [34] for 10 different initial perturbations on the border of the DoA.</i>	38
4.2.1 Example of Reference Trajectories r_i and r_j for UV_i and UV_j	42
4.3.1 Proposed Control Architecture	43
4.3.2 Feasibility Condition for Waypoint Switches	47
4.3.3 Possibility of collision between UV_i and UV_j . The possibility of collision is represented by the non-empty intersection (yellow area) between $\bigcup_{l=0}^{l_i(t)-1} \{\mathcal{T}_i^l(\bar{r}_i)\}$ (purple region) and $\bigcup_{l=0}^{l_j(t)-1} \{\mathcal{T}_j^l(\bar{r}_j)\}$ (pink region), see condition (61). . . .	49

4.3.4	The subplot (a) shows the starting connectivity graph where the node $\bar{i} = 1$ is selected to be stopped according to the procedure (P1)-(P3) and condition (63). Subplot (b) shows that in the second iteration of (P1)-(P3), the node $\bar{i} = 3$ is stopped. Finally, subplot (c), shows the final disconnected graph that guarantees absence of collisions.	50
4.4.1	Vehicles' trajectories for $t \in [0, 100]s$	57
4.4.2	Potential collision at $t = 1.5s$. Subplot [a] shows the existing intersections between the families of one-step controllable sets and the corresponding connectivity graph $\mathcal{G}(1.5)$. Subplot [b] shows the remaining collisions when UV_5 is stopped. Subplot [c] shows the absence of collision when both UV_3 and UV_5 are stopped.	57
4.4.3	Vehicles' set membership indices in the time interval $[0 - 25]s$ (left side) and zoom-in in the time interval $[0 - 3.5]s$ (right side).	61

List of Tables

3.3.1 Worst case time to transient stability (t_s^{worst}) and error for 500 simulation runs involving different initial conditions $x_i(0) \in DoA$ and disturbance $d(t)$ realizations.	37
---	----

List of Abbreviations

MPC:	Model Predictive Control
ST:	Set- Theoretic
ST-MPC :	Set-Theoretic Model Predictive Control
MIMO :	Multi-Input Multi-Output
LMI :	Linear Matrix Inequality
LP :	Linear Programming
MP :	Multi-Parametric
QP :	Quadratic Programming
DoS:	Denial of Service
UV:	Unmanned Vehicle
MUV:	Multi Unmanned Vehicle
MILP:	Mixed Integer Linear Programming
HJ:	Hamilton Jacobi
RHC:	Receding Horizon Control
DMPC:	Decentralized Model Predictive Control
LTI:	Linear Time Invariant
RCI:	Robust Control Invariant
UUB:	Uniformly Ultimately Bounded
PMU:	Phasor Measurement Unit
PFL:	Partial Feedback Linearization
ZOH:	Zero Order Hold
O1:	Objective 1
O2:	Objective2

LQR: Linear Quadratic Regulator
DoA: Domain of Attraction
TM: Traffic Manager

Chapter 1

Introduction

1.1 Literature review and motivation

Model predictive control is a Multi-Input Multi-Output (MIMO) model-based control strategy which is intrinsically capable of dealing, in the design stage, with constraints on both input command and state variables [1]. This is essential to avoid loss of performance due to the saturation effect which might occur in practical scenarios. Using the dynamic model of a plant and the available measurements, MPC predicts the future evolution of the system over a finite prediction horizon, and it solves a constrained optimization problem to select the best admissible control action that minimizes a given cost function (see Fig. 1.1.1). In simply words, MPC aims at achieving optimal performance and stability while satisfying given constraints. Fig. 1.1.2 summarizes the MPC algorithm where at each time instant k the constrained optimization problem is solved over a finite future horizon of N steps. The solution provides a sequence of $N-1$ optimal control actions where only the first control move $u^*(k|k)$ is applied to the system. At the next time steps, according to the receding horizon paradigm, such optimization is repeated on the updated state measurements.

In the MPC literature [2], it is possible to distinguish the following main classes of MPC according to the nature of the plant model, the constraints and the cost function:

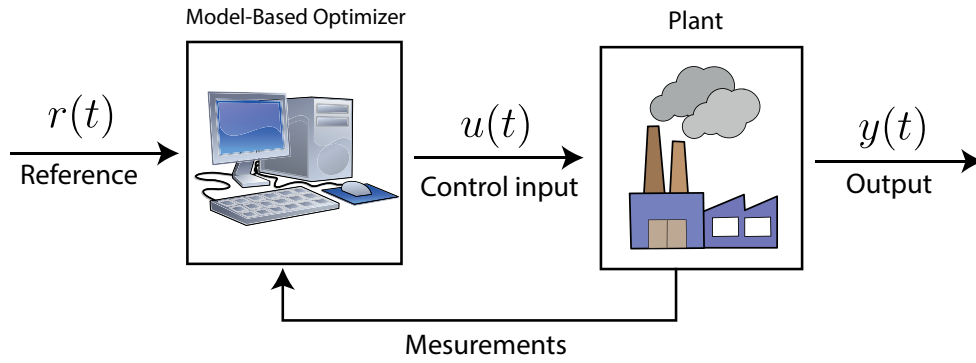


Figure 1.1.1: Basic structure of Model Predictive Control

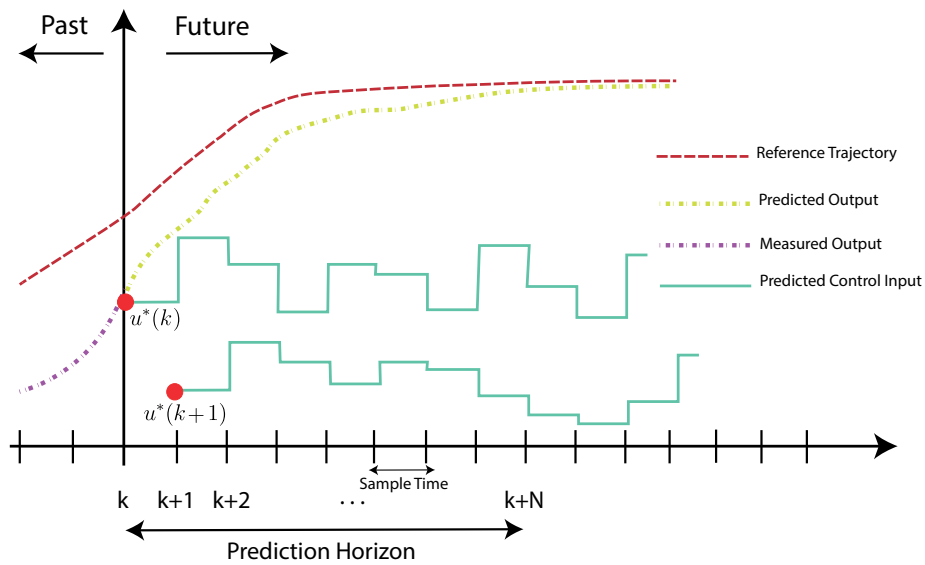


Figure 1.1.2: A discrete MPC scheme

linear MPC [3–5], non-linear MPC [6, 7], stochastic MPC [8], hybrid MPC [9], distributed MPC [10, 11], explicit MPC [12] and robust MPC [13, 14].

Of interest in this thesis are Robust MPC Solutions. Robust MPC strategies are used in the control problems where the objective is to maintain the stability and satisfy the performance properties of the system regardless of a specified range of model uncertainties and bounded disturbances [14]. In particular, the objective is to design at each time step an optimal state-feedback control action that minimizes a cost associated to the worst-case realization of the uncertainties and disturbances for systems subject to input and state constraints. The above mentioned min-max optimization problem is non-convex

and therefore difficult to solve [15]. Hence, many solutions have been proposed to recast the min-max optimization problem into a convex optimization involving Linear Matrix Inequalities (LMIs) see e.g. [3], [13], [15–18] and references therein. The tractable formulation of the min-max optimization problem was first proposed in [13], where the online min-max optimization was approximately formulated as a Linear Program (LP) for uncertainty descriptions w.r.t. the system’s impulse response. Along similar lines is [17], in which the authors developed a LP problem with a reduced number of constraints, and simple for on-line implementation. In [16] the proposed solution described the uncertainty as lower and upper bounds on impulse response coefficients, as a result the optimization problem has been cast into a LP of moderate size. Moreover, in [3] the authors optimized robust performance for polytopic/ multi-model and structured feedback uncertainties using linear programming. Polytopic uncertainty description was also used in [18] where an approximated convex formulation for optimizing the dynamic feedback control laws for constrained linear systems subject to polytopic uncertainty was presented. However, it is worth mentioning that by modeling uncertainties and disturbances as bounded polyhedron, the resulting on-line computation complexity exponentially grows with the number of vertices of the uncertainty set [3].

Indeed, the on-line computational demand for synthesizing a robust MPC algorithm limits its applicability to relatively slow and/or small problems which makes the aforementioned solutions not doable in strict real-time applications. In such regard, in the literature, different contributions have been appeared to mitigate the computational cost of robust MPC solutions. A possible way to mitigate such drawback is to completely move into an off-line phase all the required computations. Such idea is well-known as explicit MPC in which we rely on the pre-calculated solutions of the optimization for all possible problem instances which can then be used as a control look-up table on-line see e.g. [12, 19–22] and references therein. In [19] the authors obtained a piecewise linear feedback controller defined over a partition of the set of states into simplicial cones, by computing a feasible

input sequence for each vertex via linear programming. In [20] properties of the polyhedral partition of the state space has been studied which is induced by the Multi-Parametric (MP) piecewise affine solution and new MP-Quadratic Programming (QP) solver is proposed. In [21] the authors have exploited explicit MPC to deal with linear discrete-time constrained hybrid systems where the solution to the optimization problem is based on quadratic or linear performance criteria. Moreover, a new stage cost is introduced in [22] which allows one to approximate a min-max model predictive control problem with a single linear program where the authors have shown that the obtained optimal control law is piecewise affine and can be explicitly pre-computed so that the linear program does not require on-line solution. It is worth mentioning that explicit MPC approaches work well for systems with small state and input dimensions, few constraints, and short time horizons [23]. Moreover, the resulting control action might be excessively conservative.

Therefore a novel MPC solution that is based on set-theoretic arguments has been proposed as a trade off between completely on-line and completely off-line architecture [24–26]. The set-theoretic MPC reduces the typical computation burden of robust MPC controllers [27]. This is obtained by moving most of the required computations into an off-line phase, while leaving a simple and real-time affordable computational algorithm in the on-line phase.

In this thesis we have extended the ST-MPC in order to deal with two main control problems: set point regulation and reference tracking. The former is faced as a transient stability problem in smart grid systems while the latter is addressed for Multi Unmanned Vehicles (MUVs) moving in a shared planar environment where collisions must be avoided.

1.1.1 Transient Stability Control Problem

In the last decade, smart grid systems have received increasing attention. Smart grids, in general, can take advantage of bidirectional and high speed communication channels [28] as well as computation capabilities to improve performance, efficiency and reliability of

traditional power systems [29].

Power systems need to fast mitigate unexpected events such as faults and disturbances. Smart grids still face the same issues, however the available communication and computation resources allow designing novel control schemes that can outperform legacy controllers. In this contest, the transient stability control problem represents a typical case scenario where a cyber/physical attack/fault produces an impulsive perturbation in the grid.

In such circumstances, efficient control strategies are needed to fast recover stability [30], [31]. To solve such a regulation problem different solutions have been proposed in the related literature, see e.g. [32–36], and references therein.

In [32], a minimum time bang-bang controller has been proposed. In [33] the authors have proposed a distributed nonlinear controller capable of dealing with communication delays and disturbances. In [34] a parametric feedback linearization technique has been used to decouple the generator’s dynamics leading to the design of simple state feedback controllers which ensure closed-loop stability and phase cohesiveness. Along similar lines is also [35], where a delay-adaptive parametric feedback linearization technique has been used to design a delay-resilient control framework capable of contrasting Denial of Service (DoS) cyber-attacks and communication latency. Finally, in [36] a nonlinear model-free controller is proposed to address the transient stability problem in presence of delays, unmodeled dynamics and time-varying plant parameters.

It is a matter of fact that available transient stability models, as any model of physical phenomena, can only approximately describe the grid behavior. Moreover, measurement errors and disturbances can also play a significant role. Hence, control systems need to be designed to be robust against such uncertainties ensuring the satisfaction of minimum performance requirements. Furthermore, control logic should be designed taking into account limited power available for the control action, see for example the fast acting energy storage systems considered in [34]. On the basis of this reasoning and existing

state-of-the art solutions, we believe that physical limitations of smart grid subsystems and modeling errors are often underestimated. Indeed, in the controller’s design stage it is extremely important to take care of limited resources and inaccurate models to avoid performance deterioration or unexpected results caused by saturation effects [37], [38].

Moreover, to address the transient stability regulation problem in presence of disturbances, modeling errors and constraints robust MPC approaches, see e.g. [39], represent a natural solution. Nevertheless, the fast dynamics of generators might render such scheme not doable. Indeed, classical robust solutions suffer from a notable computational complexity which might prevent their applicability in fast real-time contests [1,27]. Therefore, there exists the need for computationally efficient and real-time affordable control algorithms capable of fast recovering the transient stability of the smart grid system while satisfying physical constraints on the state and/or inputs regardless of the admissible disturbances.

1.1.2 Reference tracking in Multi Unmanned Vehicle systems

As the world’s cities become more congested and polluted, new intelligent transportation models and technologies are emerging to solve the mobility challenge. One of the major technological trends is converging to autonomous driving. As a result, Unmanned Vehicles (UVs) have attracted significant attention because they have the potential to improve the traditional transportation systems in terms of congestion, emissions, and safety [40,41].

To obtain a fully automated transportation system, different issues must be addressed [42]. To name a few: each vehicle must be able to track a reference signal and reach the desired goal [43,44]; formation control tools are needed to guarantee coordination among vehicles [45–48]; and absence of collisions must be ensured [49–51].

Of particular interest for this application are control solutions capable of addressing the collision-free reference tracking control problem for multi unmanned vehicles moving in

a shared environment. Formation control approaches have been largely applied to multi-vehicle systems to address such a problem, see e.g. [45], [52–57] and references therein. However, the agents’ dynamics are often modeled as single or double integrators, and the problem is solved at a kinematic level where state and input constraints are not taken into account. Therefore, although the proposed solutions are efficient and effective, they cannot be straightforwardly adapted to deal with MUVs physical limitations or disturbances. As a result, collision avoidance cannot be guaranteed.

To address the collision avoidance problem, different strategies have been proposed. In [49], collision-free movements and deadlock-avoidance for multi-robot systems are achieved by proposing a nominal controller capable of formally fulfilling safety constraints. The safety controller is designed by defining a proper quadratic programming problem based on a mixture of relaxed control barrier functions, hybrid braking controllers, and consistent perturbations. In [58–63], different Mixed Integer Linear Programming (MILP) approaches, and model predictive control techniques have been investigated. In [58], the collision avoidance problem for a group of vehicles is formulated as an MILP optimization problem where each vehicle has an a priori known fixed number of possible trajectories. Along similar lines is also the work in [59] in which collision avoidance is ensured for a team of three vehicles, and where the exponential complexity of the obtained Hamilton-Jacobi (HJ) and MILP problems is reduced using a combinational technique based on (HJ) reachability and MILP programming concepts. In [60], a formation for a group of heterogeneous vehicles with nonlinear dynamics is achieved by applying a distributed Receding Horizon Control (RHC) strategy. The proposed solution ensures the string stability of a leader-follower platoon yet the collision avoidance problem is not explicitly considered. In [61], an MPC strategy is used to guarantee the absence of collision for a robot formation. First, feedback linearization and MPC controllers are used to recast the problem in terms of a mixed integer quadratic programming problem. Then, a branch and bound algorithm is used to reduce the complexity of the resulting optimization problem. In [62], the authors

have implemented a robust Decentralized Model Predictive Controller (DMPC) for a team of cooperating UVs where possibilities of collisions are modeled as coupling constraints. The resulting optimization problem is solved as an integer programming problem. Finally, in [63], a theoretical framework based on an MPC control paradigm is developed to methodologically ensure collision-free urban traffic by formally deriving constraints that guarantee the absence of collisions. The provided solution, although interesting, results to be conservative.

We can summarize the above state-of-art discussion as follows. Collision free-reference tracking movements cannot be assured if the trajectory planner/formation control schemes take into account only the kinematic unconstrained models of the vehicles. On the other hand, to provide a complete control solution capable of ensuring vehicles' constraints fulfillment as well as the absence of collisions, then MPC schemes represent a natural choice. Nevertheless, the resulting control approaches might be either conservative or computationally demanding.

1.2 Thesis Contribution

In this thesis the ST-MPC control paradigm is used to solve a robust regulation problem in smart grid and robust tracking problem with collision avoidance in multi unmanned vehicle systems. The proposed control schemes are capable of ensuring the desired control objectives while satisfying input/ state constraints regardless of admissible disturbance realizations.

For the transient stability control problem, we have proposed a MPC controller [64] which can robustly cope with model uncertainties and physical limitations. In a nutshell, the proposed controller consists of two feedback actions: the first performs a partial feedback compensation of the nonlinear dynamical coupling among generators, while the second exploits set-theoretic arguments to robustly achieve transient stability in spite of non perfect decoupling, disturbances and physical limitations of the fast acting energy storage

system. In what follows we have proved that the robust transient stability is guaranteed and the worst-case time to transient stability is finite and a-priori known. Moreover, to better highlight the capabilities of the proposed scheme, we have contrasted the proposed solution with a competitor scheme presented in [34] by means of a solid simulation example.

In the multi-vehicle application, we have extended the ST-MPC to deal with the reference tracking control problem for a system of heterogeneous MUVs moving in a shared environment [65]. We have considered a scenario where each vehicle follows a trajectory imposed by a local planner and where each UV can have different linear dynamics as well as different constraints and disturbances. In this contest, we have designed a novel control architecture where a centralized traffic manager, in conjunction with ad-hoc designed local vehicle controllers, is capable of ensuring the absence of collisions. The proposed solution has been obtained by exploiting, for the local vehicles' controllers, a dual-mode MPC and, for the traffic manager, the set-theoretic and controllability properties. Moreover, after modeling the potential vehicle collisions with a graph, connectivity arguments have been used to obtain an optimal collision avoidance resolution which minimizes the number of vehicles that need to be stopped. We have proved that, regardless of the local reference signals, the resulting control scheme ensures collision-free signal tracking. Simulation results, conducted on a system of five vehicles, have been shown to provide tangible evidence of the features of the proposed framework.

It is worth mentioning that in both examples, the controllers are capable of reducing the computational burden of the typical MPC schemes since most of the required computations are moved into an offline phase leaving into the online phase a simple and real-time affordable optimization problem.

1.3 Thesis Layout

The manuscript is organized as follows:

- Chapter 2: First, the main concepts and definitions used along the thesis are defined. Then, the basic ST-MPC control paradigm is summarized.
- Chapter 3: A Set-Theoretic Model Predictive Control Approach for Transient Stability in Smart Grid is presented.
- Chapter 4: A Guaranteed Collision Free Reference Tracking in Constrained Multi Vehicle Systems is designed.
- Chapter 5: The conclusions as well as the possible directions for future work are presented.

1.4 Publications

- **Maryam Bagherzadeh**, Shima Savehshemshaki and Walter Lucia. “Guaranteed Collision-Free Reference Tracking in Constrained Multi Unmanned Vehicle Systems”, Under review for Automatica journal.
- [66] **Maryam Bagherzadeh** and Walter Lucia. “A Model Predictive Set-Theoretic Control Approach for Transient Stability in Smart Grid”, 2019 IET Control Theory and Applications journal.
- [65] **Maryam Bagherzadeh** and Walter Lucia. “Multi-Vehicle Reference Tracking with Guaranteed Collision Avoidance” 2019 IEEE European Control Conference (ECC).
- [64] Lucia Walter, Kian Gheitasi, and **Maryam Bagherzadeh**. “A Low Computationally Demanding Model Predictive Control Strategy for Robust Transient Stability in Smart Grid” 2018 IEEE Conference on Decision and Control (CDC).

Chapter 2

Background on Set-Theoretic MPC

The intent of this chapter is to provide the necessary background material for the understanding of the rest of the manuscript. In particular, the basic ingredients (one-step controllable sets, positively invariant region, etc.) needed to design a dual-mode set-theoretic MPC controller are revisited. Then, the off-line and online phases of the set-theoretic MPC are summarized and the main properties of set-theoretic control paradigm are highlighted. Finally, the chapter ends summarizing the computational algorithm.

2.1 Preliminaries and Definitions

We consider systems described by the discrete-time linear time-invariant (LTI) representation

$$x(t+1) = Ax(t) + Bu(t) + d(t) \tag{1}$$

subject to input and state constraints:

$$u(t) \in \mathcal{U}, \quad x(t) \in \mathcal{X}, \quad \forall t \geq 0, \tag{2}$$

with additive bounded exogenous disturbances:

$$d(t) \in \mathcal{D} \subset \mathbb{R}^d, \quad 0_d \in \mathcal{D} \quad (3)$$

where $t \in \mathbb{Z}_+ := \{0, 1, \dots\}$ is the sampling time instants, $u \in \mathbb{R}^m$ the control input, $x \in \mathbb{R}^n$ the state space vector, and A and B are matrices of suitable dimensions characterizing the system's dynamical behavior. Moreover, $\mathcal{U} \subseteq \mathbb{R}^m$ and $\mathcal{X} \subseteq \mathbb{R}^n$ are compact subsets with $0_m \in \mathcal{U}$ and $0_n \in \mathcal{X}$, respectively. It is worth noticing that sets \mathcal{U} , \mathcal{X} and \mathcal{D} are polyhedra.

Definition 1. (*RCI*) A set $\mathcal{T} \subseteq \mathcal{X}$ is said **robust control Invariant set** for the linear constrained system (1)-(3) if

$$\forall x \in \mathcal{T} \rightarrow \exists u \in \mathcal{U} \quad \text{s.t.} \quad Ax + Bu + d \in \mathcal{T}, \quad \forall d \in \mathcal{D}, \forall t \in \mathbb{Z}_+ \quad (4)$$

Definition 2. For the linear constrained system (1) under disturbance realization (3) the **robust one-step controllable set** to the set \mathcal{T} is defined as:

$$Pre(\mathcal{T}) = \{x \in \mathbb{R}^n : \exists u \in \mathcal{U} \text{ s.t. } Ax(t) + Bu + d(t) \in \mathcal{T}, \forall d \in \mathcal{D}\} \quad (5)$$

$Pre(\mathcal{T})$ is the set of states which evolve into the target set \mathcal{T} in one time step regardless of admissible disturbances.

Definition 3. For a given target set $\mathcal{T} \subseteq \mathcal{X}$, the **N -step controllable set** (\mathcal{T}^N) of the system (1) subject to the constraints (2) is defined recursively as:

$$\mathcal{T}^l = Pre(\mathcal{T}^{l-1}) \cap \mathcal{X}, \quad \mathcal{T}^0 = \mathcal{T}, \quad l = \{1, 2, \dots, N\} \quad (6)$$

Based on Definition.3, the set \mathcal{T}^0 , defines all the initial conditions, $x(0)$, that can be steered in at most N steps within \mathcal{T}^0 by applying a suitable control sequence, while satisfying input and state constraints.

Definition 4. Given two sets $\mathcal{P} \subseteq \mathbb{R}^n$ and $\mathcal{Q} \subseteq \mathbb{R}^n$, the **Pontryagin/ Minkowski Set Difference** $\mathcal{P} \sim \mathcal{Q}$ and **Set Sum** $\mathcal{P} \oplus \mathcal{Q}$ are defined as

$$\begin{aligned}\mathcal{P} \sim \mathcal{Q} &:= \{x \in \mathbb{R}^n : x + q \in \mathcal{P}, \forall q \in \mathcal{Q}\} \\ \mathcal{P} \oplus \mathcal{Q} &:= \{p + q \mid p \in \mathcal{P}, q \in \mathcal{Q}\}\end{aligned}\tag{7}$$

Definition 5. [24] (**Uniformly Ultimately Bounded**) Let $\mathcal{Q} \subset \mathbb{R}^n$ be a neighborhood region of the origin. The closed-loop trajectory of (1), is said to be *Uniformly Ultimately Bounded (UUB)* in \mathcal{Q} if for all $\mu > 0$, there exists $T(\mu) > 0$ such that $\forall \|x(0)\| \leq \mu \rightarrow x(t) \in \mathcal{Q} \forall d_i(t) \in \mathcal{D}_i$ and $\forall t \geq T(\mu)$.

2.2 Set-Theoretic Model Predictive Control (ST-MPC)

Given an equilibrium pair (x^{eq}, u^{eq}) for the disturbance-free plant (1), we design a dual-mode robust MPC controller which is capable of stabilizing the state trajectory $x(t)$ in a neighborhood of x^{eq} regardless of disturbances (3) and constraints (2). The off-line and online steps needed to design the controller are summarized.

In the off-line phase the following 3 steps must be performed:

Off-line:

Step 1: Considering the unconstrained disturbance-free model of (1), we design a stabilizing state-feedback control law,

$$u(t) := K(x - x^{eq}) + u^{eq}\tag{8}$$

to asymptotically steer the plant state trajectory to the equilibrium x^{eq} [67]. Such a controller is hereafter referred as the terminal controller.

Step 2: The smallest RCI region, namely \mathcal{T}^0 , associated to the terminal controller

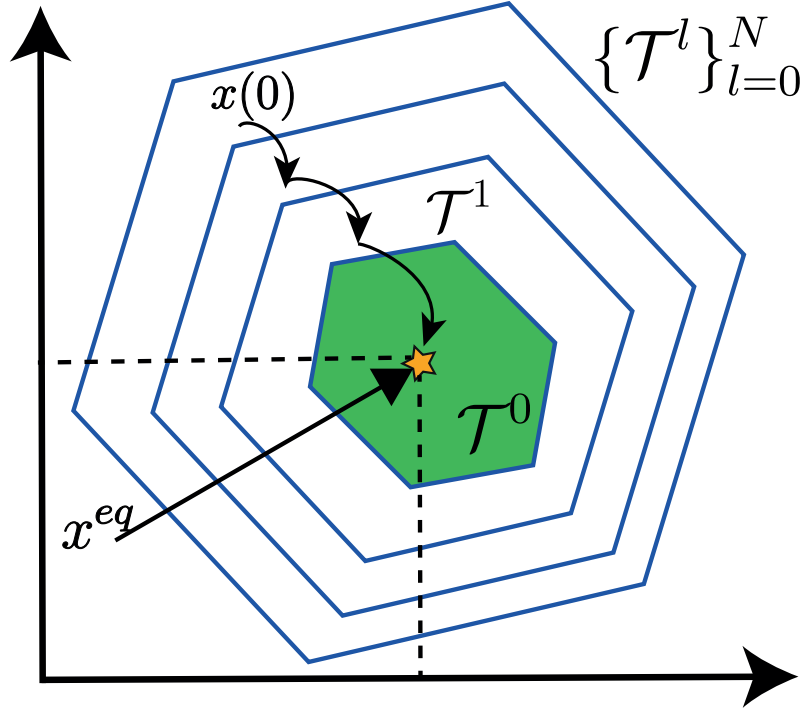


Figure 2.2.1: N-step controllable family set

is computed as proposed in [68] under the requirement:

$$\mathcal{T}^0 \subseteq \mathcal{X}, u(t) \in \mathcal{U}, \quad \forall t. \quad (9)$$

The region \mathcal{T}^0 is hereafter referred as the terminal region (see the green region in Fig. 2.2.1).

Step 3: The controller computed in Steps 1-2 might have a very small domain. To ensure that any initial state $x(0)$ belongs to the controller admissible region, we can enlarge the domain by computing a family of robust one-step controllable sets, namely $\{\mathcal{T}^l\}_{l=0}^N$, $N \geq 1$, by applying the following recursive definition [24]:

$$\begin{aligned} \mathcal{T}^l &:= \{x \in \mathcal{X} : \exists u \in \mathcal{U} : \forall d \in \mathcal{D}, Ax + Bu + d \in \mathcal{T}^{l-1}\} \\ &= \{x \in \mathcal{X} : \exists u \in \mathcal{U} : Ax + Bu \in \tilde{\mathcal{T}}^{l-1}\} \end{aligned} \quad (10)$$

where $\tilde{\mathcal{T}}^{l-1} := \mathcal{T}^{l-1} \sim \mathcal{D}$ and N is the number of computed sets. The set union

$\bigcup_{l=0}^N \{\mathcal{T}^l\}$ defines the final controller domain of attraction, namely DoA . Fig. 2.2.1 shows e.g. the family of one-step controllable sets built for a LTI system with two states where $\bigcup_{l=0}^N \{\mathcal{T}^l\}$ presents the DoA of the controller.

In the online phase, the off-line built family of one-step controllable set, is exploited to compute the control action u to minimize the desired cost function $J(x(t), u)$. In particular,

Online:

Step 1: Find the smallest set index $l(t)$ containing $x(t)$, i.e.

$$l(t) := \min\{l \leq N : x(t) \in \mathcal{T}^l\}$$

Step 2: If $l(t) = 0$ i.e. $x(t) \in \mathcal{T}^0$, apply the control action given by terminal controller (8), otherwise apply the control input obtained from the solution of the following optimization problem:

$$\begin{aligned} u(t) = \arg \min_u J(x(t), u) \quad s.t. \\ Ax(t) + Bu \in \tilde{\mathcal{T}}^{l(t)-1} \end{aligned} \tag{11}$$

It is worth mentioning that for varied control problems $J(x(t), u)$ can be chosen to minimize different performance indices such as (i) time to converge to the equilibrium point or (ii) control effort. In particular, if fast convergence is of interest then $J(x(t), u) = \|Ax(t) + Bu\|_2^2$, if control effort is preferred then $J(x(t), u) = \|u\|_2^2$. If both objectives (i)-(ii) are of interest then any convex combination of the above can be considered.

2.2.1 Properties

It is possible to prove that the described set-theoretic control paradigm enjoys the following properties:

- For all x_0 in the family of one-step controllable sets $\bigcup_{l=0}^N \{\mathcal{T}^l\}$, the plant's state vector evolution, $x(t)$, converges to the terminal region \mathcal{T}^0 in maximum N steps.
- The trajectory is Uniformly Ultimately Bounded (UUB) in \mathcal{T}^0 regardless of any disturbance realization $d(t)$.
- In the absence of disturbance the equilibrium x^{eq} will be asymptotically reached in virtue of the stabilizing nature of the control laws associated to the terminal region.

2.3 ST-MPC Computation Algorithms

The above developments are collected into the following computational algorithm.

Set-Theoretic MPC (ST-MPC)

————— **off-line phase** —————

Output: $\bigcup_{l=0}^N \mathcal{T}^l$

- 1: Compute an RCI region \mathcal{T}^0 and the associated control function see (8).
- 2: Compute a family of N robust one-step controllable sets according to the recursion (10).
- 3: Store $\{\mathcal{T}^l\}_{l=0}^N$

————— **online phase** —————

Input: $\{\mathcal{T}^l\}_{l=0}^N, x(0) \in \bigcup_{l=0}^N \mathcal{T}^l$

Output: $u(t)$

- 1: Find the smallest set index $l(t)$ containing $x(t)$, i.e.

$$l(t) := \min_{l \in \{0, \dots, N\}} l \text{ s.t. } x(t) \in \mathcal{T}^l$$

2: **if** $l(t) = 0$ **then**

▷ **We are in RCI.**

 Compute $u(t) := K(x - x^{eq})$.

3: **else** Solve the convex optimization problem

$$u(t) = \arg \min_u J(x(t), u) \quad s.t. \quad (12)$$

$$Ax(t) + Bu \in \tilde{\mathcal{T}}^{l(t)-1}, \quad u \in \mathcal{U} \quad (13)$$

4: **end if**

5: Apply to (1) the control action $u(t)$.

6: $t \leftarrow t + 1$ goto Step 1

Chapter 3

A Set-Theoretic Model Predictive Control Approach for Transient Stability in Smart Grid

In this chapter, an ST-MPC based control technique is designed to address the transient stability control problem in Smart Grid systems. The proposed MPC controller is capable of robustly recovering the effect of physical/ cyber state perturbation of the linear constrained system.

This work is published in IET Control Theory and Applications journal and is partially published in the IEEE Conference on Decision and Control (CDC), 2018 [64], [66].

3.1 Problem Formulation

We consider a smart grid consisting of L agents [69] organized as in Fig. 3.1.1. Each agent has four main components:

- A Generator;
- A Phasor Measurement Unit (PMU) that measures generator rotor angle and its

with $\delta_i(t)$ the rotor angle, $\omega_i(t) = (\omega_i^{act} - \omega_0)$ the angular speed deviation of the angular rotor speed ω_i^{act} w.r.t. the nominal speed ω_0 , H_i the generator inertia, D_i the damping coefficient, and $u_i(t)$ the control input provided by an external power source. Moreover,

$$P_i^a = P_i^m - P_i^e \quad (15)$$

is defined as the difference between the mechanical P_i^m and electrical P_i^e power of the generator i , and P_i^e is computed as

$$P_i^e = \sum_{k=1}^N |E_i| |E_k| G_{ik} [\cos(\delta_i - \delta_k) + B_{ik} \sin(\delta_i - \delta_k)] \quad (16)$$

where G_{ik} and B_{ik} are the transfer conductance and susceptance between generators i and k . Furthermore, E_i is the internal voltage of the generator i which is obtained from the solution of the differential equation

$$\dot{E}_i = -\frac{1}{T_i} [E_i + (X_{di} - X'_{di})i_{di} - E_{fi}] \quad (17)$$

where X_{di} is the direct-axis reactance of the generator, X'_{di} is the direct-axis transient reactance of the generator and T_i is the open circuit transient time constants. To ensure phase cohesiveness, each generator needs to work around a nominal equilibrium configuration, namely $x_i^{eq} = [\delta_i^*, 0]^T$, which satisfies the following requirement

$$|\delta_i^* - \delta_j^*| \leq 100, \quad \forall (i, j), \text{ s.t. } i \neq j.$$

In addition, the power system is considered transiently stable when starting from a post-fault initial state $x_i(0)$, the state of the i -th generator converges to the equilibrium point x_i^{eq} [72], [73]. By considering disturbances and model uncertainties, transient stability is considered achieved when for each i -th generator, the state variable ω_i becomes confined withing a polytope Ξ_i^{ts} shaping an admissible error region around the desired equilibrium

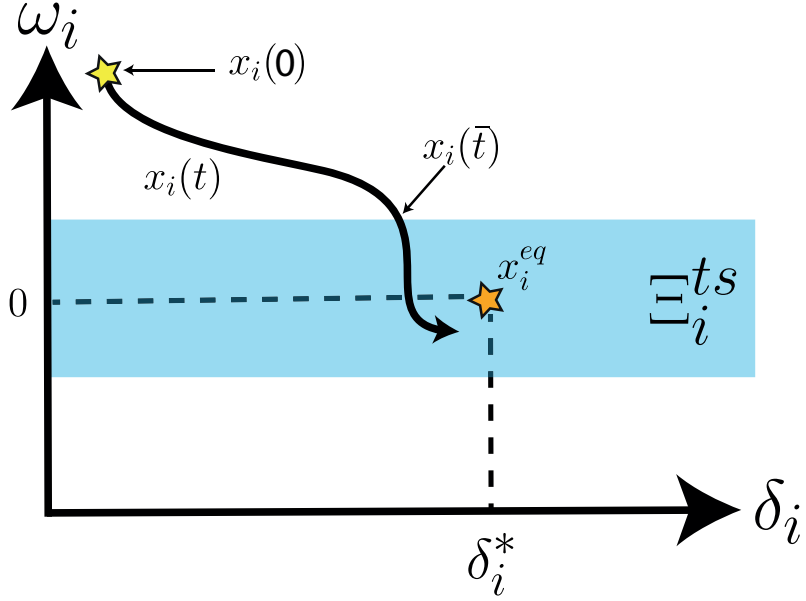


Figure 3.1.2: *Generator i : Transient Stability Region.*

[36] (see the light blue rectangular region in Fig. 3.1.2). The transient stability region is modeled as follows

$$\Xi_i^{ts} := \{\omega_i \in \mathbb{R} : |\omega_i| \leq \varepsilon_\omega\} \quad (18)$$

where $\varepsilon_\omega > 0$ is the tolerance level.

In order to model the dynamics of the generators properly, we need to take into account existing physical limitations on the external power source, modeling errors and disturbances.

In particular, the following are defined:

- Maximum deliverable power $\bar{P}_i^s < \infty$ on $u_i(k)$:

$$|u_i(k)| < \bar{P}_i^s, \quad \forall k \quad (19)$$

- Measurement errors on the state variables δ_i and ω_i and imperfect dynamical coupling on P_i^a :

$$\begin{bmatrix} \delta_i(k) \\ \omega_i(k) \end{bmatrix} = \begin{bmatrix} \delta_i^*(k) \\ \omega_i^*(k) \end{bmatrix} + d_i^m(k) \quad (20)$$

$$P_i^a = P_i^{a*}(k) + e_{P_i^a}(k)$$

where $\delta_i^*(t)$, $\omega_i^*(t)$ and P_i^{a*} are the actual values and

$$d_i^m(k) := \begin{bmatrix} e_{\delta_i}(k) \\ e_{\omega_i}(k) \end{bmatrix} \in \mathcal{D}_i^m, \quad \forall k, \quad \text{and} \quad e_{P_i^a}(k) \in \mathcal{D}_i^{P_a}, \quad \forall k \quad (21)$$

defines the measurement error vectors constrained within the bounded polyhedral set $\mathcal{D}_i^m \subseteq \mathbb{R}^2$, $0_2 \in \mathcal{D}_i^m$ and $\mathcal{D}_i^{P_a} \subseteq \mathbb{R}$, $0_1 \in \mathcal{D}_i^{P_a}$, characterizing the component-wise bounds

$$|e_{\delta_i}(k)| \leq \bar{e}_{\delta_i}, \quad |e_{\omega_i}(k)| \leq \bar{e}_{\omega_i}, \quad |e_{P_i^a}(k)| \leq \bar{e}_{P_i^a}, \quad \forall k \quad (22)$$

- Dynamical model (14) errors:

$$\begin{bmatrix} \dot{\delta}_i(k) \\ \dot{\omega}_i(k) \end{bmatrix} = \begin{bmatrix} \dot{\delta}_i^*(k) \\ \dot{\omega}_i^*(k) \end{bmatrix} + d_i^p(k) \quad (23)$$

where $\dot{\delta}_i^*(t)$ and $\dot{\omega}_i^*(t)$ describe the ideal dynamical model and

$$d_i^p(k) \in \mathcal{D}_i^p, \quad \forall k \quad (24)$$

with $0_2 \in \mathcal{D}_i^p \subset \mathbb{R}^2$ a bounded polyhedral disturbance set.

Without loss of generality, we discretize the agents model (14) and we describe the i -th agent dynamics (14)-(22) with the following uncertain discrete-time representation:

$$\begin{cases} x_i(k+1) = A_i x_i(k) + B_i(u_i(k) + P_i^{a*}(k)) + G_p d_i^p(k) \\ y_i(k) = x_i(k) + d_i^m(k) \end{cases} \quad (25)$$

subject to the input constraint

$$|u_i(k)| \leq \bar{P}_i^s \quad (26)$$

and disturbances

$$d_i^p(k) \in \mathcal{D}_i^p, \quad d_i^m(k) \in \mathcal{D}_i^m, \quad e_{P_i^a}(k) \in \mathcal{D}_i^{P_a} \quad (27)$$

where $x_i(k) = [\delta_i, \omega_i]^T$ is the state vector and $y(k) = [\delta_i, \omega_i]^T$ the measurement vector. In addition,

$$A_i = e^{A_i T_s}, \quad B_i = \left(\int_0^{T_s} e^{A_i(T_s - \tau)} d\tau \right) B_i, \quad \text{and} \quad G_p = T_s I_2 \quad (28)$$

and T_s is the sampling time.

Remark 1. *It is worth mentioning that, due to the digital nature of PMU, sensors measurements need to be sampled prior to communication. Hence, the Partial Feedback Linearization (PFL) controller receives further frequent updates on the generator states $x_i(t)$ as the value of T_s is decreased. In order to take into account the effect of the value of T_s , the control action u_i is implemented in a step-wise manner. In particular, it is possible to assume it as a function of $\delta(nT_s)$ and $\omega(nT_s)$ for the time interval $t = [nT_s, (n+1)T_s]$ when $n \in N_+ = \{1, 2, \dots\}$ [34]. Nevertheless, any discretization model is accepted and is practical while considering appropriate sampling time that matches the selected method. In this chapter, the discrete model is obtained using Zero Order Hold (ZOH) method.*

The control problem addressed in this chapter can be formally stated as follows:

Robust Transient Stability in Smart Grid: *Given the Smart Grid architecture shown in Fig. 3.1.1, the constrained uncertain generators' model (25)-(27), the post-fault initial state $x_i(0)$, the desired equilibrium configurations $x_i^{eq} = [\delta_i^*, 0]^T$, and the transient stability admissible regions Ξ_i^{ts} . Design a distributed state feedback control law*

$$u_i(k) := \eta_i(y_i(k), x_i^{eq}), \quad \forall i \quad (29)$$

capable of achieving the following objective:

- **(O1)-Robust and Predictable Transient Stability:** *In a finite number of steps, $t_s < \infty$, each generator i must be robustly confined within the transient stability region Ξ_i^{ts} regardless of any admissible disturbance realization (27) while preserving the constraints (26). Moreover, in the absence of disturbances, asymptotic stability of the equilibrium state x_i^{eq} must be ensured.*

3.2 Proposed Controller

Traditionally, in Smart Grid systems, synchronous generators are controlled by resorting to the *governor control* paradigm [74] to ensure that undesired state perturbations (e.g. the effect of an impulsive state disturbance) will be rejected. However, the resulting closed-loop system usually exhibits a slow stabilization settling time and, as a consequence, it cannot efficiently deal with large perturbations [34].

In this chapter, we propose a novel distributed MPC-based controller capable of ensuring robust and fast transient stability in spite of model uncertainties and disturbances. The proposed control action is given by the sum of two contributions, i.e.

$$u_i(k) := u_i^f(k) + u_i^c(k) \quad (30)$$

where:

- $u_i^f(k)$ performs a partial feedback compensation of the dynamical coupling term P_i^{a*} among the agents;
- $u_i^c(k)$ ensures robust post-fault transient stability in spite of non perfect cancellation of the coupling term, disturbances and measurement noise, see (20)-(23).

In what follows, for feasibility reasons, we assume that the fast-acting generators can provide a power \bar{P}_i^s greater than \bar{P}_i^a , i.e.

$$\bar{P}_i^s >:= \bar{P}_i^a, \quad \bar{P}_i^a := \max |P_i^a| \quad (31)$$

The latter is instrumental for ensuring that the control action $u_i(k)$ is sufficiently strong to contrast the coupling effect between generators.

In the next sections, first the control actions $u_i^f(k)$ and $u_i^c(k)$ will be justified and designed, and then the complete computational control algorithm is summarized.

3.2.1 Controller for Partial Coupling Compensation (u_i^f)

In smart grid systems we can take advantage of the existing communication infrastructure (Fig. 3.1.1) and phasor measurement units (PMUs) to partially compensate the coupling terms P_i^{a*} so rendering the closed-loop dynamical model (25) decoupled [34]. This strategy recalls the well-known feedback linearization technique [75] which, over the last three decades, has been widely used for excitation control in smart grid applications, see e.g. [71, 76–78] and references therein.

We design the control action $u_i^f(k)$ as:

$$u_i^f(k) = -P_i^a \quad (32)$$

where P_i^{a*} is the best available estimation of P_i^a , see (20). As a consequence, $u_i^f(k)$ performs a partial imperfect cancellation of the coupling term between generators. By substituting $u_i^f(k)$ into (25) we obtain an uncertain dynamical model where the effect of the coupling term consists of the measurement error $e_{P_i^a}(k)$, i.e.

$$x_i(k+1) = A_i x_i(k) + B_i u_i^c(k) + B_i e_{P_i^a}(k) + G_p d_i^p(k) \quad (33)$$

where

$$|u_i^c(k)| \leq \bar{U}_i^c \quad (34)$$

and $\bar{U}_i^c := \bar{P}_i^s - \bar{P}_i^a$.

3.2.2 Set-theoretic controller for Robust Transient Stability (u_i^c)

The objective of the control action u_i^c can be stated as follows: given the constrained and uncertain generator model (33)-(34), design a state-feedback control action $u_i^c(k)$ capable of achieving transient stability (**O1**) in spite of imperfect coupling cancellation (32) and disturbance realizations (27).

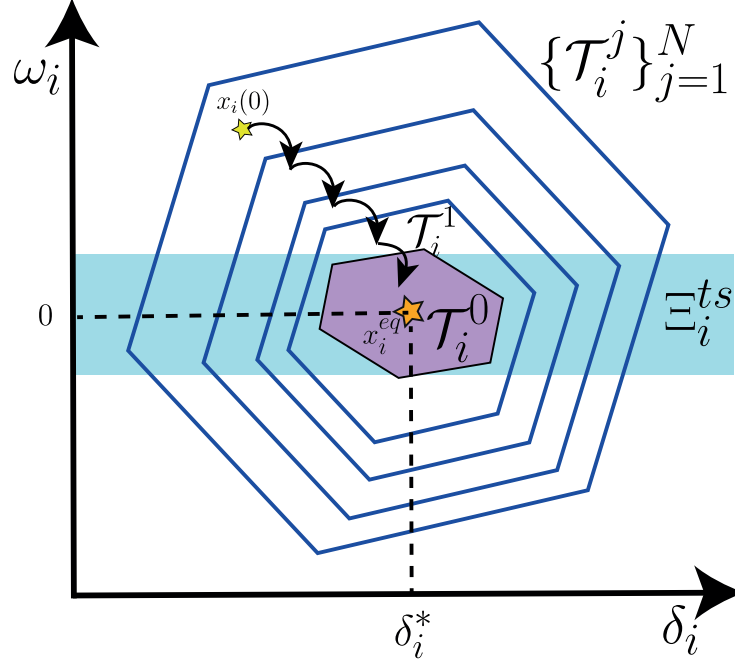


Figure 3.2.1: Transient stability region Ξ_i^{ts} (blue rectangular region), RCI terminal region \mathcal{T}_i^0 (purple polyhedron), Family of robust one-step controllable sets $\{\mathcal{T}_i^j\}_{j=1}^N$ (blue polyhedra). Moreover, $x_i(0)$ is the initial perturbation and the black arrows show the state trajectory obtained from the proposed controller.

We here propose a robust controller which is based on the low computationally complex set-theoretic MPC control scheme [25], [26]. In particular, the proposed controller is a dual-mode set-theoretic controller [25] which consists of: (i) a terminal robust control invariant (RCI) region (see *Definition 1*) and (ii) a family of robust one-step controllable sets (see *Definition 2*). Please refer to Fig. 3.2.1 for a graphical illustration of the RCI region (purple polyhedron) and one-step controllable sets (family of blue polyhedron).

(i)-*Robust Control Invariant Region*. We would like to recall that transient stability is achieved when the state trajectory is confined within Ξ_i^{ts} , i.e.

$$x(k) \in \Xi_i^{ts}, \quad \forall t \geq \bar{t}, \quad \bar{k} \leq \infty \quad (35)$$

Therefore, it would be desirable to have a control action $u_i^c(k)$ for (33)-(34) capable of

confining the generator state trajectory within an RCI region contained in (18) regardless of any admissible disturbance (27) realization, see e.g. the region \mathcal{T}_i^0 in Fig. 3.2.1. The latter can be achieved by first designing a state feedback stabilizing control law $u_i^c(k) = g(x_i(k), x_i^{eq})$ on the disturbance-free dynamical model (33) and then computing the associated minimal RCI region as proposed in [39] under the requirement

$$\mathcal{T}_i^0 \subseteq \Xi_i^{ts}, \quad u^c(k) \in \bar{\mathcal{U}}_i^c \quad (36)$$

Therefore, by construction, for any $x_i(0) \in \mathcal{T}_i^0$, the controller $u_i^c(k) = g(x_i(k), x_i^{eq})$ fulfills the objective **(O1)**.

Remark 2. *A simple way to design the state-feedback controller $u_i^c(k) = g(x_i(k), x_i^{eq})$ is by resorting to the well-known Linear Quadratic Regulator (LQR):*

$$u_i^c(k) = K_i(x_i(k) - x_i^{eq}) + u_i^{eq} \quad (37)$$

where $K_i \in \mathbb{R}^{m \times n}$ is the LQR gain and the pair (u_i^{eq}, x_i^{eq}) represents the desired equilibrium configuration.

Remark 3. *It is worth noticing that the designed controller has a limited domain of attraction (DoA). Therefore, we need to enlarge its operation region in order to deal with severe transient stability perturbations $x_i(0) \notin \mathcal{T}_i^0$. In what follows, we increase the controller DoA by resorting to robust one-step controllable sets. \square*

(ii)-Family of Robust One-Step Controllable Sets

By exploiting the concept of one-step robust controllable sets (see *Definition 2*), we can enlarge the RCI region \mathcal{T}_i^0 by means of a family $\{\mathcal{T}_i^j\}_{j=1}^N$ of $N < \infty$ robust one-step controllable sets computed recursively applying the following definition (see Fig. 3.2.1):

$$\begin{aligned} \mathcal{T}_i^j := \{y_i \in \mathbb{R}^n : \exists u \in \bar{\mathcal{U}}_i^c \text{ s.t. } A_i y_i + B_i u_c^i + B_i e_{P_i^a} + G_p d_i^p \in \mathcal{T}_i^{j-1}, \\ \forall e_{P_i^a} \in \mathcal{D}_i^{P_i^a}, d_i^a \in \mathcal{D}_i^a\} \end{aligned} \quad (38)$$

It is important to underline that the use of the measurement vector $y(k)$ (instead of $x_i(t)$) is instrumental to take care of unavoidable sensor measurement errors (20), i.e.

$$\begin{aligned} \mathcal{T}_i^j := \{x_i \in \mathbb{R}^n : \exists u \in \bar{\mathcal{U}}_i^c \text{ s.t. } A_i(x_i + d_i^m) + B_i u_c^i + B_i e_{P_i^a} + G_p d_i^p \in \mathcal{T}_i^{j-1}, \\ \forall e_{P_i^a} \in \mathcal{D}_i^{P_a}, d_i^a \in \mathcal{D}_i^a, d_i^m \in \mathcal{D}_i^m\} \end{aligned} \quad (39)$$

By taking advantage of the Pontragin/Minkowski difference and sum operators we can remove the worst case realization of the uncertainties from \mathcal{T}_i^{j-1} and obtain

$$\mathcal{T}_i^j = \{x \in \mathbb{R}^n : \exists u_c^i \in \bar{\mathcal{U}}_i^c \text{ s.t. } A_i x_i + B_i u_c^i \in \tilde{\mathcal{T}}_i^{j-1}\} \quad (40)$$

where $\tilde{\mathcal{T}}_i^{j-1} := \mathcal{T}_i^{j-1} \sim (G_p \mathcal{D}_i^p \oplus B_i \mathcal{D}_i^{P_a} \oplus A_i \mathcal{D}_i^m)$.

Remark 4. *In the literature, different algorithms [24] and toolboxes [79] have been developed to numerically compute exact [80] or approximated [81] robust one-step controllable sets (40). \square*

Given a family of robust one-step controllable sets, the following result holds true:

Proposition 1. *The set union*

$$\bigcup_{j=0}^N \mathcal{T}_i^j \quad (41)$$

defines an RCI region for (33)-(34) regardless of any admissible disturbance realization.

Proof. Let us consider an initial post-fault state $x_i \in \mathbb{R}^n$ such that $x_i \in \bigcup_{j=0}^N \mathcal{T}_i^j$. Then, there exists $\bar{j} \leq N$ such that $x_i \in \mathcal{T}_i^{\bar{j}}$. Moreover, according to (40) there exists an admissible command input $u_c^i \in \bar{\mathcal{U}}_i^c$ capable of steering the predicted one-step system evolution, namely x_i^+ , within the successor set $\tilde{\mathcal{T}}_i^{\bar{j}-1}$. As a consequence, the following logical implication, by construction, holds true:

$$x_i^+ \in \tilde{\mathcal{T}}_i^{\bar{j}-1} \implies x_i(t+1) \in \mathcal{T}_i^{\bar{j}-1}, \quad \forall e_{P_i^a} \in \mathcal{D}_i^{P_a}, d_i^a \in \mathcal{D}_i^a, d_i^m \in \mathcal{D}_i^m \quad (42)$$

According to *Definition 1*, this is sufficient to guarantee that $\bigcup_{j=0}^N \mathcal{T}_i^j$ is an RCI region for (33)-(34). \square

Finally, at each time instant k , the control law associated to the RCI region (41) is obtained from the solution of the following convex optimization problem:

$$u_i^c = \arg \min_u J(y_i(k), u) \quad s.t. \quad (43)$$

$$A_i y_i(k) + B_i u \in \tilde{\mathcal{T}}_i^{\bar{j}-1}, \quad u \in \bar{\mathcal{U}}_i^c \quad (44)$$

where $J(y_i(k), u)$ is a convex cost function.

Remark 5. *For transient stability purposes, $J(y_i(k), u)$ can be chosen to minimize different performance indices such as (i) the time to achieve transient stability or (ii) the control effort. In particular, if fast transient stability is of interest then $J(y_i(k), u) = \|A_i y_i(k) + B_i u\|_2^2$, if the control effort is preferred then $J(y_i(k), u) = \|u\|_2^2$. If both indices (i)-(ii) are of interest then any convex combination of the above can be considered, e.g. $J(y_i(k), u) = \alpha \|A_i y_i(k) + B_i u\|_2^2 + \beta \|u\|_2^2$, with $\alpha + \beta = 1$, $\alpha > 0, \beta > 0$. It is important to notice that, regardless of the chosen performance index $J(y_i(k), u)$, condition (42) is always fulfilled.*

3.2.3 Computational Algorithm and Controller Properties

In this section, first all the above developments are collected into a computational algorithm, then the controller effectiveness and properties are stated.

Generator i , Set-Theoretic MPC (ST-MPC)

————— **off-line phase** —————

Output: $\bigcup_{j=0}^N \mathcal{T}_i^j$

- 1: Compute an RCI region \mathcal{T}_i^0 satisfying (36) and the associated control function $u_i^c(k) = g(x_i(k), x_i^{eq})$, see (58).
- 2: Compute a family of N robust one-step controllable sets according to the recursion (40), see **Remark 4**.
- 3: Store

$$\{\mathcal{T}_i^j\}_{j=0}^N$$

————— **online phase** —————

Input: $\{\mathcal{T}_i^j\}_{j=0}^N, y_i(0) \in \bigcup_{j=0}^N \mathcal{T}_i^j$

Output: $u_i(k)$

- 1: Compute $u_i^f(k)$ according to (32)
- 2: Find the smallest set index $j(k)$ containing $y_i(k)$, i.e.

$$j(k) := \min_{j \in \{0, \dots, N\}} j \quad s.t. \quad y_i(k) \in \mathcal{T}_i^j$$

3: **if** $j(k) = 0$ **then**

▷ **terminal region**

4: Compute $u_i^c(k) = K_i(y_i(k) - x_i^{eq}) + u_i^{eq}$

5: **else** Solve the convex optimization problem

$$u_i^c(k) = \arg \min_u J(y_i(k), u) \quad s.t. \tag{45}$$

$$A_i y_i(k) + B_i u \in \tilde{\mathcal{T}}_i^{j(k)-1}, \quad u \in \bar{\mathcal{U}}_i^c \tag{46}$$

6: **end if**

7: Apply

$$u_i(k) = u_i^f(k) + u_i^c(k)$$

8: $k \leftarrow k + 1$ goto Step 1

Proposition 2. *Given the generator uncertain models (25)-(27), the families of one-step controllable sets $\bigcup_{j=1}^{N_i}\{T_i^j\}, \forall i$, computed according to (40), and an initial generator perturbation $x_i(0) \in \bigcup_{j=0}^N \mathcal{T}_i^j, \forall i$, then the **ST-MPC** algorithm achieves the objective (O1). In particular:*

- $x_i(k) \in \Xi_i^{ts}, \forall k \geq \bar{k}$ with $\bar{k} \leq N < \infty$;
- In the absence of disturbances ($d_i^m \equiv 0, d_i^p \equiv 0, e_{P_i^a} \equiv 0$), x_i^{eq} is an asymptotically stable equilibrium point;
- The resulting online control algorithm requires the solution of simple and real-time affordable convex quadratic programming problem under linear constraints.

Proof. First, it is important to notice that, by construction, the presence of the feedback compensation term u_i^f assures that each generator locally behaves according to the model (33)-(34). Therefore, *Proposition 1* guarantees that the state trajectory of each generator is, in the worst case, confined within the controller domain of attractions, i.e. $x_i(k) \in \bigcup_{j=0}^N \mathcal{T}_i^j, \forall k$. This ensures that we can always find a controllable set containing the current state vector $x_i(k)$, see $j(k)$ in Step 2 of the **ST-MPC**-online phase. As a consequence, the optimization problem (45)-(46) always admits a solution and the index set $j(k)$ must exhibit, over time, a monotonically decreasing behavior which guarantees that the terminal region \mathcal{T}_i^0 is reached in at most $N < \infty$ time steps irrespective of any admissible initial perturbation $x(0)$ and disturbance realization. Therefore, since $\mathcal{T}_i^0 \forall i$ are RCI regions contained within the transient stability and phase cohesiveness regions Ξ_i^{ts} , i.e. $\mathcal{T}_i^0 \subseteq \Xi_i^{ts}, \forall i$, we have that

$$\forall i \implies x_i(k+N) \in \Xi_i^{ts}, \forall k \geq 0$$

In the time domain, the above translates in the fact that the time to transient stability is upper bounded by the worst case t_s^{worst} defined as

$$t_s^{worst} := NT_s \tag{47}$$

Moreover, in the absence of disturbances, $d_i^m \equiv 0$, $d_i^p \equiv 0$, $e_{P_i^a} \equiv 0$ the equilibria x_i^{eq} will be asymptotically reached in virtue of the stabilizing nature of the control laws associated to the terminal region, see Step 4 of the **ST-MPC**-online phase.

Finally, it is worth to notice that most of the required computations have been moved into the off-line phase of the **ST-MPC**, leaving into the online phase a simple and real-time affordable control algorithm. Indeed, the main computational complexity of the online phase is represented by the convex Quadratic Programming (QP) optimization problem (45) over the linear constraints (46). \square

3.3 Simulation

In this section, the effectiveness of the proposed solution is shown. Furthermore, the achieved control performance are compared, both in terms of robustness and time required to achieve transient stability, with the solution in [34]. The New England 10-generator 39-bus smart grid shown in Fig.3.1.1 has been used as the test-bed system. The system has been emulated within the Matlab environment using the grid parameters in [69]. In addition, the MPT3 toolbox [79] has been used to implement the **ST-MPC** algorithm.

Based on Remark.1, the stability time of the system generators increases if the value of T_s increases. In the simulation examples it is shown that the proposed control strategy is capable of stabilizing the generators within few seconds even when the sampling time is selected as large as 0.2 sec. Therefore, the dynamical model of each generator has been discretized using a sampling time of $T_s = 0.2$ sec. According to the system model description (25).

$$A_i = \begin{bmatrix} 1 & 0.200 \\ 0 & 0.997 \end{bmatrix}, \quad B_i = \begin{bmatrix} 0.0075 \\ 0.0755 \end{bmatrix}$$

We assume that the available fast action storage system imposes the following constraint on the maximum available power u_i^c :

$$|u_i^c| \leq 6 \text{ p.u.} \quad (48)$$

Hereafter, for sake of simplicity and to better understand the properties of the proposed controller, only the performance of a single generator, namely i , is shown. By considering the generator model centered around the equilibrium configuration x_i^{eq} , the transient stability problem reduces to a simple regulation to zero. According to the robust one-step controllable set definition (40), we can define different levels of uncertainties by considering their cumulative effect $d(k)$ given by the following Minkowski set sum:

$$d(t) \in \mathcal{D} \subseteq \mathbb{R}^2, \text{ with } \mathcal{D} := G_p \mathcal{D}_i^p \oplus B_i \mathcal{D}_i^{Pa} \oplus A_i \mathcal{D}_i^m$$

The following bounds are considered on the disturbance level $d(t)$

$$|d_1(t)| \leq 0.50 \quad |d_2(t)| \leq 0.60, \quad \forall t$$

The transient stability region is chosen to be

$$\Xi_i^{ts} := \{\omega \in \mathbb{R} : |\omega_i| \leq 0.8\},$$

which correspond to a normalized rotor speed within the range of 0.2%.

We have performed an intensive simulation campaign to contrast the controller in [34] with the proposed **ST-MPC** for different initial perturbation $x_i(0)$ and different disturbance realizations. However, to better underline the *modus operandi* of the proposed solution, the simulation results for a single generator are depicted .

According to the **ST-MPC** off-line phase, first an RCI region (\mathcal{T}_i^0) has been computed exploiting the algorithm developed in [68], then a family of one-step controllable set has

been obtained to cover the region of admissible initial perturbations.

$$DoA := \bigcup_{j=0}^{219} \{\mathcal{T}_i^j\}$$

Please refer to Fig. 3.3.3 for a graphical representation of the controller's DoA.

The proposed **ST-MPC** controller is contrasted with the solution in [34] for which the following design parameters have been chosen

$$\alpha_i = 2.5, \quad \beta_i = 0.8$$

and a saturation effect, capable of imposing the actuator constraint (48), has been added.

The two strategies are compared in Figs. 3.3.1-3.3.4 both in terms of time to transient stability and robustness. In Fig. 3.3.1, a comparison based on a single run is shown. In particular, we consider an initial perturbation equal to $x_i(0) = [-50, 15]^T \in \mathcal{T}_i^{92}$, on the i -th generator where the rotor angle δ_i , if expressed in the range $[-\pi, +\pi]$, corresponds to $-5\pi/36$ rad. The resulting generator state trajectories are depicted in Fig. 3.3.1. It is possible to appreciate that the **ST-MPC** controller is capable of steering the state trajectories within the transient stability region $\Xi_i^{ts} \supset \mathcal{T}_i^0$ in 6.3sec while the control strategy proposed in [34] requires 12.8sec. The main advantage of the **ST-MPC** controller become clearer in Fig. 3.3.2 where also the control signal $u_i^e(t)$ is shown. In particular, it is possible to notice that the proposed controller is capable of better using the constraint on the maximum deliverable power (48). This is testified by the fact that control commands in **ST-MPC** saturate at an earlier stage w.r.t the ones of [34]. This experimental result confirms that, differently from [34], the **ST-MPC** controller has been conceived to explicitly and optimally take care of the generator constraints and disturbances.

In Table 3.3.1, we compare the two strategies according to the following performance indices:

- Worst case transient stability time t_s^{worst} . In each run, the transient stability time t_s

is defined as:

$$t_s := \min_{t \in \mathbb{Z}_+} t \text{ s.t. } x(t) \in \Xi_i^{ts} \forall t \geq t_s^{worst}$$

- Worst case average transient stability error e_s^{worst} . In each run, the average transient stability error e_s is defined as:

$$e_s := \frac{\sum_{k=0}^{N_p} |(x_i(k) - x_i^{eq})|}{N_p}$$

where $N_p = 800$ is the number of steps used in the simulation.

In particular, we have considered 500 runs with random disturbance realizations and initial conditions. The numerical results in Table 3.3.1 show that the proposed controller is capable of achieving transient stability with a time and an error that are, in the worst case, roughly half of the one obtained by [34]. Moreover, for **ST-MPC**, the worst case time $\bar{t}_s^{worst} = 29.2$ sec, validate the theoretical bound defined in (47), i.e. $t_s^{worst} = T_s * 219 = 43.8$ sec .

Finally, in Figs. 3.3.3 and 3.3.4 the results are shown for 10 selected initial perturbations lying on the border of the controller domain of attraction (see Fig. 3.3.3).

Fig. 3.3.3 shows the generator state trajectories obtained for **ST-MPC** while Fig. 3.3.4 contrast **ST-MPC** with [34] showing the worst case time to transient stability. Moreover, in Fig. 3.3.4 it is possible to appreciate that using the algorithm in [34], trajectory overshoots are possible for some initial conditions. On the other hand, the **ST-MPC** controller avoid this undesired phenomena by design. This last consideration justifies why the time to transient stability are notably reduced with the **ST-MPC** controller.

3.4 Conclusion

In this chapter, we have proposed a novel set-theoretic MPC controller that can optimally and robustly deal with the transient stability control problem in Smart Grid. We have

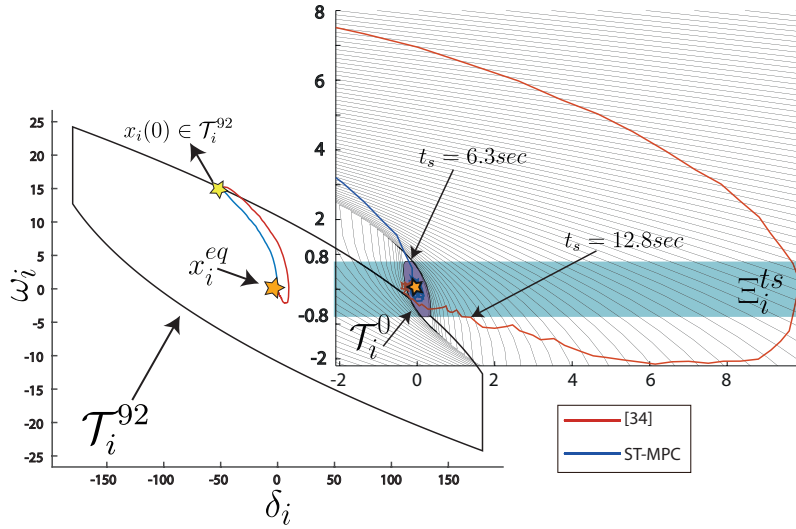


Figure 3.3.1: i -th generator state trajectory $x_i(t)$ for $x_i(0) = [-50, 15]$.

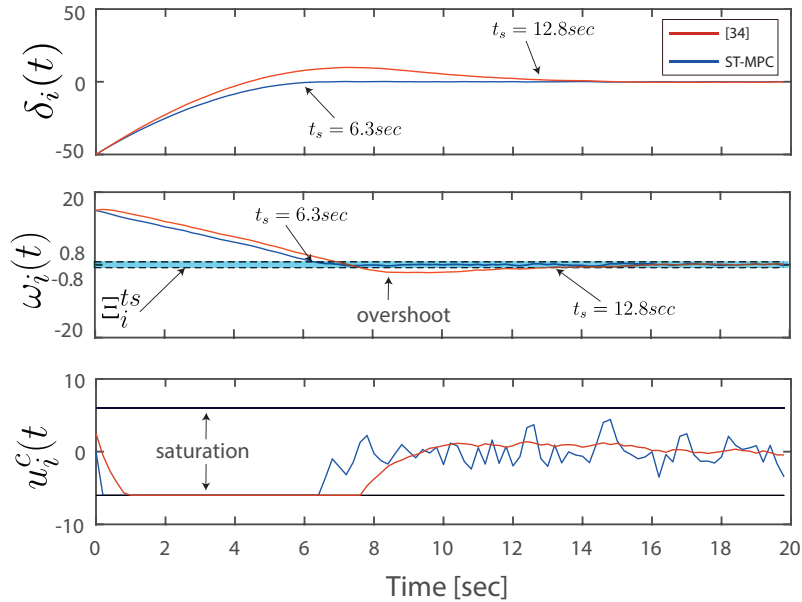


Figure 3.3.2: Rotor angle $\delta_i(t)$, Rotor angular speed $\omega_i(t)$ and Command Input $u_i^c(t)$: ST-MPC vs [34].

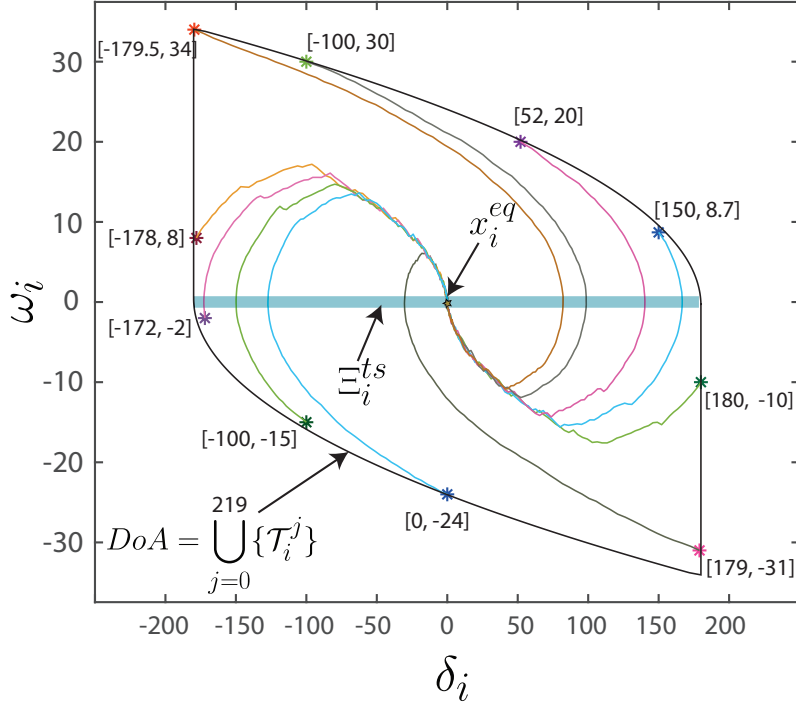


Figure 3.3.3: *ST-MPC Domain of Attraction (DoA) and i -th generator state trajectories $x_i(t)$ for 10 different initial perturbations on the border of the DoA.*

formally proved that a worst-case bound on the recovery time exists and it can be guaranteed using the proposed **ST-MPC** controller. Finally, by means of simulation experiment, we have shown that the proposed controller can achieve better performance with respect to a recent competitor scheme. As future work, the authors would like to extend the proposed scheme to deal with more severe cyber-attack scenarios that might affect in a more persistent way the communication channels.

	<i>Worst Case</i>	ST-MPC	[34]
Transient stability time t_s^{worst} [sec]		29.2	51.5
Transient stability avg. error e_s		146.9	338.8

Table 3.3.1: *Worst case time to transient stability (t_s^{worst}) and error for 500 simulation runs involving different initial conditions $x_i(0) \in DoA$ and disturbance $d(t)$ realizations.*

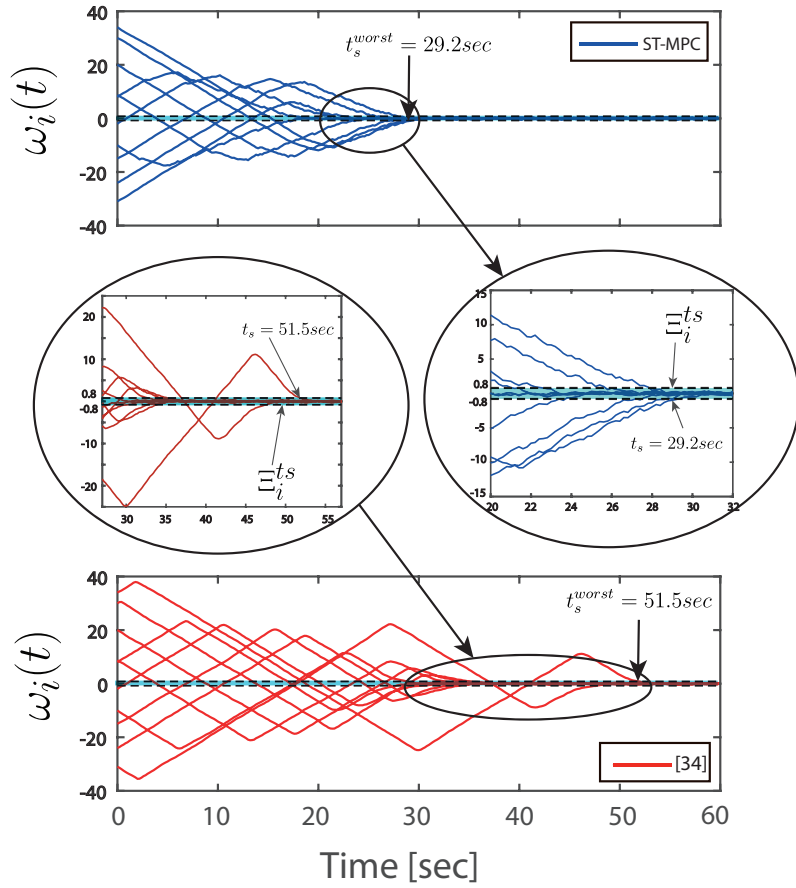


Figure 3.3.4: Rotor angular speed $\omega_i(t)$: ST-MPC vs [34] for 10 different initial perturbations on the border of the DoA.

Chapter 4

Guaranteed Collision Free Reference Tracking in Constrained Multi Vehicle Systems

In this chapter, the ST-MPC based controller is extended to deal with the reference tracking with collision avoidance control problem for a system of heterogeneous Multi Unmanned Vehicles (MUVs) moving in a shared environment [65]. The vehicles are required to follow a trajectory imposed by a local planner and each UV can have different linear dynamics as well as different constraints and disturbances.

This work is currently under review in the Automatica journal and is partially published as a conference paper in the IEEE European Control Conference CC, 2019 [65].

4.1 Preliminaries and definitions

Definition 6. (*Absence of Collisions*) *Let's consider a pair (i, j) of UVs. In what follows, we assume absence of collisions between the vehicles i and j if*

$$\|p_i(t) - p_j(t)\|_2 > 0, \quad \forall t \in \mathbb{Z}_+ \quad (49)$$

Definition 7. [82] (**Graph**) An undirected graph is an ordered pair $\mathcal{G} = (\mathcal{V}, \mathcal{E})$ where \mathcal{V} is the vertex (or node) set and \mathcal{E} is edge set which is defined as a finite subset of all admissible unordered pairs in \mathcal{V} , i.e. $\mathcal{E} \subset \{e_{uv} := \{u, v\} : u, v \in \mathcal{V}\}$.

Definition 8. [82] (**Adjacency Matrix**) Given an undirected graph $\mathcal{G} = (\mathcal{V}, \mathcal{E})$, the adjacency matrix $\mathcal{A}[\mathcal{G}]$ is a squared symmetric matrix such that

$$\mathcal{A}[\mathcal{G}]_{ij} = \begin{cases} 1 & \text{if } e_{uv} \in \mathcal{E} \\ 0 & \text{otherwise} \end{cases} \quad (50)$$

Definition 9. [82] (**Degree Matrix**) Given an undirected graph \mathcal{G} , the adjacency degree of each vertex $v_i \in \mathcal{V}$, namely $d(v_i)$, is given by the number of vertices $v_j \in \mathcal{V}$ connected to v_i with an edge, i.e. $(v_i, v_j) \in \mathcal{E}$. The degree matrix $\Delta[\mathcal{G}]$ is defined as the diagonal matrix containing the adjacency degrees for all the vertices, i.e.

$$\Delta[\mathcal{G}] = \begin{pmatrix} d(v_1) & 0 & \cdots & 0 \\ 0 & d(v_2) & \cdots & 0 \\ \vdots & \vdots & \ddots & \vdots \\ 0 & \cdots & 0 & d(v_n) \end{pmatrix} \quad (51)$$

Definition 10. [82] (**Completely Disconnected Graph**) A graph \mathcal{G} is said completely disconnected when each element in the degree matrix $\Delta[\mathcal{G}]$ is zero.

4.2 Problem Formulation

In this section, first, the considered scenario and assumptions are explained, then the problem formulation is stated.

Considered Scenario: We suppose a set $\mathcal{I} := \{1, 2, \dots, S\}$ of S heterogeneous unnamed vehicles moving in a two-dimensional planar environment of coordinates $p_i = [p_i^x, p_i^y]^T$ and described by the class of constrained discrete-time linear time-invariant (LTI) systems

with additive bounded exogenous disturbances. Each i -th UV must follow a reference trajectory, namely $\mathbf{r}_i \in \mathbb{R}^2$, provided by a high-level reference generator.

Assumption 1. *We assume that the dynamical model of each i -th UV is described by (1)-(2) indexed by i . Where $x_i = [p_i^T, z_i^T]^T \in \mathbb{R}^{n_i}$ is the state space vector with $z_i \in \mathbb{R}^{n_i-2}$ the vector of non-spatial state-space variables (e.g., vehicle velocities). A_i, B_i are matrices of suitable dimensions characterizing the UV_i dynamical behavior, C_i is a matrix which selects the spatial components p_i from the state-vector x_i . However, UVs can have different dynamical behaviors (A_i, B_i, C_i) and/or different constraints and disturbance levels ($\mathcal{X}_i, \mathcal{U}_i, \mathcal{D}_i$). $\mathcal{U}_i \subseteq \mathbb{R}^{m_i}$ and $\mathcal{X}_i = \mathbb{R}^2 \times \mathcal{Z}_i$ where $\mathcal{Z}_i \subseteq \mathbb{R}^{n_i-2}$.*

Assumption 2. *We assume that the UVs reference generators modules are decoupled and that the trajectory planning is done at a kinematic level without taking into account the complete vehicles' model, constraints, and disturbances. Moreover, the reference generators provide the trajectories \mathbf{r}_i to the vehicles as a sequence of waypoints $r_i(k_i) \in \mathbb{R}^2$ indexed by $k_i \in \mathbb{Z}_+$, see Fig 4.2.1. We assume there exists a maximum distance $\delta_i > 0$ between two successive points, i.e. $\|r_i(k_i + 1) - r_i(k_i)\|_2 \leq \delta_i$.*

Assumption 3. *We assume that there are no communications among vehicles, but each vehicle is able to share information with a common centralized unit hereafter referred to as the traffic manager.*

Remark 6. *In the sequel, we use the discrete index t to denote the discrete-time evolution of the vehicles' variable, e.g. $x_i(t)$, $u_i(t)$, and $p_i(t)$, while we use the index k_i to denote the k_i -th waypoint $r_i(k_i)$ generated by the reference generator.*

The control problem addressed in this chapter can be stated as follows:

UVs Reference Tracking with Guaranteed Collision Avoidance: Given a set \mathcal{I} of S heterogeneous unnamed vehicles which models are described by (1)-(2):

- **(O1)** Design decentralized state-feedback controllers

$$u_i(t) := f_i(x_i(t), r_i(k_i)) \quad (52)$$

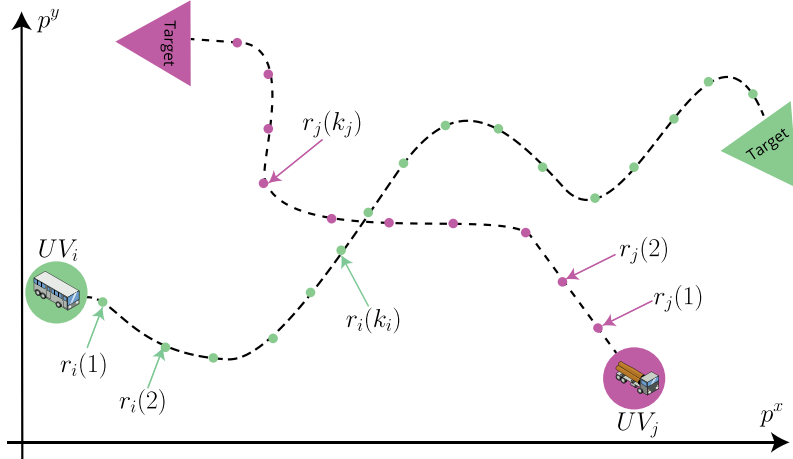


Figure 4.2.1: Example of Reference Trajectories r_i and r_j for UV_i and UV_j .

fulfilling constraints (2) despite disturbance realizations (3) and able to sequentially track the waypoints $r_i(k_i), \forall k_i$, with a tracking error that, for each waypoint, is UUB in a finite number of steps.

- **(O2)** Design a centralized traffic manager module capable of guaranteeing absence of collisions among vehicles, i.e.

$$\|p_i(t) - p_j(t)\|_2 > 0, \quad \forall t \in \mathbb{Z}_+, \quad \forall (i, j), \quad i \neq j, \quad i, j \in \mathcal{I} \quad (53)$$

regardless of the reference trajectories $\mathbf{r}_i, i \in \mathcal{I}$

4.3 Proposed Solution

In this section, a solution to the control problems **(O1)**-**(O2)** is presented. The proposed control architecture illustrated in Fig. 4.3.1 consists of:

- A set of S set-theoretic model predictive controllers (**ST-MPC**) which take care of the tracking problem **(O1)**;
- A centralized Traffic Manager (**TM**) that solves the collision avoidance problem **(O2)**.

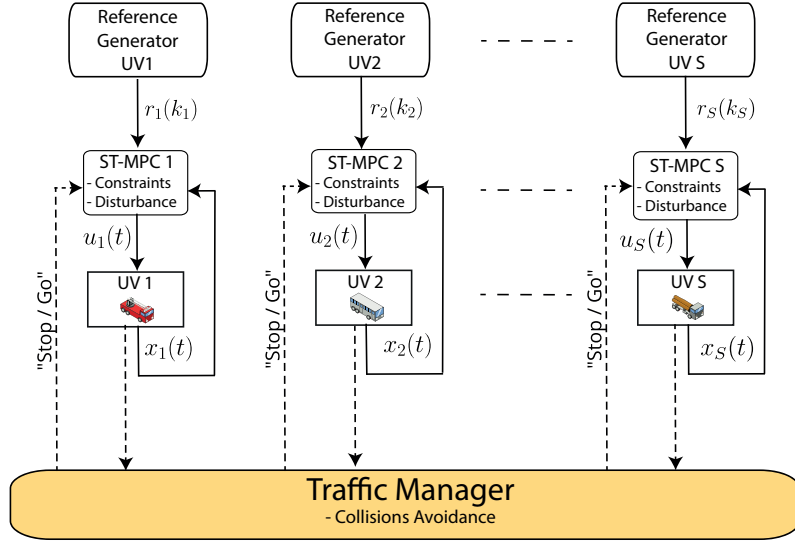


Figure 4.3.1: Proposed Control Architecture

4.3.1 Set-Theoretic MPC Tracking Controller

In this subsection, we provide a solution to the control objective **(O1)**. Our approach is based on the dual-mode set-theoretic MPC paradigm inspired by the works done in [25], and [26]. The choice for such a scheme is mainly motivated by the willingness to use an MPC algorithm which is at the same time robust, computationally efficient, and real-time affordable. Indeed, set-theoretic control is well-known for being able to move most of the required computations into an offline phase leaving into the online phase a simple computational algorithm, see [24].

The proposed tracking control strategy consists of two main actions: *(i)* regulation towards the current waypoint $r_i(k_i)$ and *(ii)* waypoint update $r_i(k_i) \rightarrow r_i(k_i + 1)$.

(i) Regulation towards the current waypoint: Let's first consider the i -th UV and a waypoint $r_i(k_i)$. In the absence of disturbances acting on (1), for any point $r_i(k_i) \in \mathbb{R}^2$, we can find the corresponding state and input equilibrium pair $(x_{r_i(k_i)}^{eq} = [r_i^T(k_i), 0_{n_i-2}]^T, u_{r_i(k_i)}^{eq} = 0)$. A robust-state feedback controller stabilizing the vehicle state trajectory $x_i(t)$ in a neighborhood of $x_{r_i(k_i)}^{eq}$ while taking care of disturbances (3) and constraints (2), can be

built along the same line of the dual-mode controller proposed in [25]. The control policy is built offline and then online exploited to compute at each sampling time the control actions. The offline and online steps are here summarized:

Offline:

(Off-1) By considering the unconstrained disturbance-free model of (1), design a stabilizing state-feedback control law,

$$u_i(t) := f_i^0(x_i(t), x_{r_i(k_i)}^{eq}) \quad (54)$$

to asymptotically bring the plant state trajectory to the equilibrium $x_{r_i(k_i)}^{eq}$. Such a controller is hereafter referred to as the terminal controller.

(Off-2) The smallest RCI region, namely $\mathcal{T}_i^0(r_i(k_i))$, associated to the terminal controller is computed as proposed in [68] under the requirements $\mathcal{T}_i^0(r_i(k_i)) \subseteq \mathcal{X}_i$, $u_i(t) \in \mathcal{U}_i, \forall t$. The region \mathcal{T}_i^0 is hereafter referred to either as the terminal region or as the domain of attraction of the terminal controller, namely DoA_i^0 .

(Off-3) The controller computed in Steps 1-2 might have a very small domain. To ensure that any initial state $x_i(t)$ belongs to the controller admissible region, the DoA_i must be enlarged. The latter is here achieved by computing a family of N_i robust one-step controllable sets, namely $\{\mathcal{T}_i^l\}_{l=0}^{N_i}$, $N_i \geq 1$, by applying the following recursive definition [24]:

$$\begin{aligned} \mathcal{T}_i^l &:= \{x_i \in \mathcal{X}_i : \exists u_i \in \mathcal{U}_i : \forall d_i \in \mathcal{D}_i, A_i x_i + B_i u_i + d_i \in \mathcal{T}_i^{l-1}\} \\ &= \{x_i \in \mathcal{X}_i : \exists u_i \in \mathcal{U}_i : A_i x_i + B_i u_i \in \tilde{\mathcal{T}}_i^{l-1}\} \end{aligned} \quad (55)$$

where $\tilde{\mathcal{T}}_i^{l-1} := \mathcal{T}_i^{l-1} \sim \mathcal{D}_i$ and N_i is the number of computed sets. The set union $\bigcup_{l=0}^{N_i} \{\mathcal{T}_i^l\}$ defines the final controller domain of attraction, namely DoA_i

Online:

(On-1) Let $x_i(t)$ be the current vehicle i 's state space vector, find the smallest set index $l_i(t)$ containing $x_i(t)$, i.e.

$$l_i(t) := \min\{l : x_i(t) \in \mathcal{T}_i^l(r_i(k_i))\} \quad (56)$$

(On-2) If $l_i(t) = 0$ (i.e. $x_i(t) \in \mathcal{T}_i^0$) apply the control action given by terminal controller (54), otherwise apply the control action give by the solution of the following quadratic programming (QP) optimization problem:

$$\begin{aligned} u_i(t) = \arg \min_{u_i \in \mathcal{U}_i} & \|A_i x_i(k) + B_i u_i - x_{r_i(k_i)}^{eq}\|_2^2 \text{ s.t.} \\ & A_i x_i(t) + B_i u_i \in \tilde{\mathcal{T}}_i^{l_i(t)-1}(r_i(k_i)) \end{aligned} \quad (57)$$

By construction, it can be straightforwardly proved that the above controller, is capable of robustly steering, in a finite number of steps, the state trajectory in the terminal region \mathcal{T}_i^0 , while fulfilling state and input constraints. Moreover, \mathcal{T}_i^0 is the RCI region where the tracking error is UUB confined, and its size represents the maximum tracking error we can commit while tracking the waypoints $r_i(k_i)$. Further details and properties of set-theoretic control can be found in [25]. In what follows, a remark is given to clarify, from a practical point of view, how the steps *(Off-1)* and *(Off-3)* can be computed.

Remark 7. *In step (Off-1), the only requirement for the state-feedback controller $u_i^0(t) := f_i^0(x_i(t), x_{r_i(k_i)}^{eq})$ is to ensure asymptotic stability for the disturbance and constraint free vehicle dynamical model (1). As a consequence, any existing state-feedback controller can be employed. In the computation algorithm shown in Section 4.3.3, we have used a linear state-feedback controller where the controller gain K_i^0 is the optimal gain given by the Linear Quadratic Regulator (LQR):*

$$u_i(t) = K_i^0(x_i(t) - x_{r_i(k_i)}^{eq}) \quad (58)$$

In step (Off-3), the robust one-step controllable sets (55) can be built using the capability offered by the MPT Matlab toolbox [79]. Nevertheless, in the literature, different algorithms exist to compute exact or approximated robust one-step controllable sets, see e.g. [24, 80, 81], and references therein. \square

(ii) Waypoint update

Let's consider $r_i(k_i)$ as the current waypoint for the i -th UV and let's assume that the previously presented set-theoretic controller has terminal region and robust one-step controllable sets centered in $r_i(k_i)$, namely $\{\mathcal{T}_i^l(r_i(k_i))\}_{l=0}^{N_i}$. We assume that it is possible to switch to the next waypoint $r_i(k_i+1)$ if and only if the terminal of the current waypoint has been reached. This assumption is without loss of generality, and it is made only to assure that the vehicle could track each waypoint with an error which is UUB bounded.

Let denote with $\bar{t} \in \mathbb{Z}_+$ the generic time instant when we want to switch to the successive waypoint $r_i(k_i+1)$. In principle, for linearity, we can switch waypoint and controller's DoA by simply re-centering the terminal region $\mathcal{T}_i^0(r_i(k_i))$ and the family of robust one-step controllable sets around the new equilibrium point $x_{r_i(k_i+1)}^{eq}$ associated to $r_i(k_i+1)$. Nevertheless, to guaranty that this operation is doable and preserves the vehicles' constraints (2), the following condition must be satisfied

$$x_i(\bar{t}) \in \bigcup_{l=0}^{N_i} \mathcal{T}_i^l(r_i(k_i+1)), \quad \forall x_i(\bar{t}) \in \mathcal{T}_i^0(r_i(k_i)) \quad (59)$$

Indeed, condition (59) ensures that any state inside the current terminal region belongs to the DoA_i of the shifted controller. Therefore, to assure waypoint switching feasibility we need to investigate the minimum domain $DoA_i(r_i(k_i+1)) = \bigcup_{l=0}^{N_i} \mathcal{T}_i^l(r_i(k_i+1))$ that satisfies the condition (59).

Proposition 3. *Let's consider the i -th vehicle model (1)-(2), the maximum distance δ_i between two successive waypoints $r_i(k_i)$ and $r_i(k_i+1)$, the terminal RCI regions $\mathcal{T}_i^0(r_i(k_i))$ and $\mathcal{T}_i^0(r_i(k_i+1))$, and the switching time instant $\bar{t} \in \mathbb{Z}_+$. A controller, with domain of*

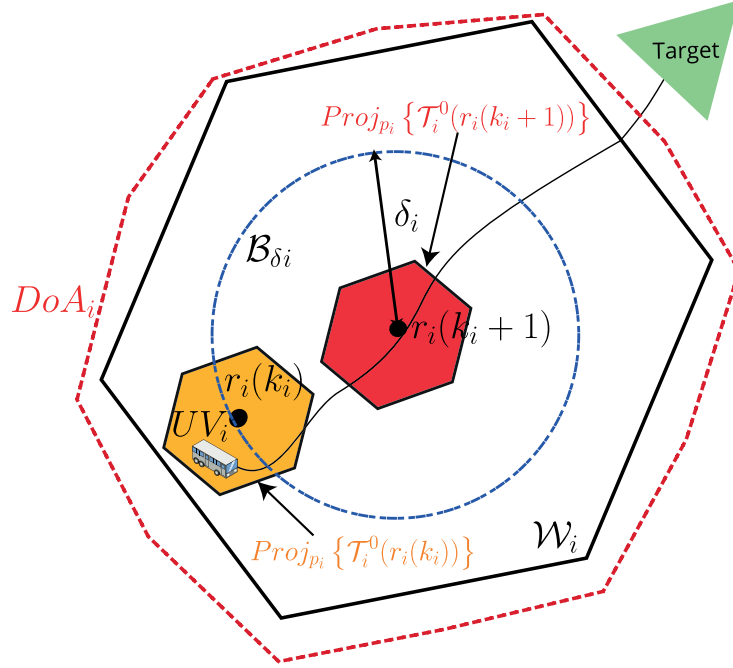


Figure 4.3.2: Feasibility Condition for Waypoint Switches

attraction $DoA_i(r_i(k_i + 1))$ guarantees condition (59) if the following set-inclusion holds true:

$$DoA_i(r_i(k_i + 1)) \supseteq \mathcal{B}_{\delta_i}(r_i(k_i + 1)) \oplus \mathcal{T}_i^0(0_2) := \mathcal{W}_i \quad (60)$$

Proof. First, to better clarify the proof, we shall refer to Fig. 4.3.2 where the considered situation is illustrated. According to *Assumption 2*, the maximum distance between two successive waypoints $r_i(k_i)$ and $r_i(k_i + 1)$ is bounded by the ball \mathcal{B}_{δ_i} . Moreover, since $\mathcal{T}_i^0(r_i(k_i))$ is an RCI region, if $x_i(t) \in \mathcal{T}_i^0(r_i(k_i))$ then the state trajectory is confined within the terminal region $\forall \bar{t} > t$. As a consequence, $DoA_i(r_i(k_i + 1))$ must cover the state-space region shaped by \mathcal{B}_{δ_i} , i.e. $\mathcal{B}_{\delta_i}(r_i(k_i + 1))$ plus $\mathcal{T}_i^0(0_2)$. Therefore, the condition $\forall x_i(\bar{t}) \in \mathcal{T}_i^0(r_i(k_i)) \rightarrow x_i(\bar{t}) \in DoA_i(r_i(k_i + 1))$ is trivially satisfied if the $DoA_i(r_i(k_i + 1))$ is bigger or equal of the subset $\mathcal{W}_i \subset \mathbb{R}^n$, defined as follows:

$$\mathcal{W}_i := \mathcal{B}_{\delta_i}(r_i(k_i + 1)) \oplus \mathcal{T}_i^0(0_2)$$

□

From the above result, we can conclude that the dual-mode controller can be used for tracking purpose as long as we can increase its DoA_i to satisfy condition (60). The latter can be simply achieved by using (60) as the stopping criteria for the recursion (55).

At this point, by collecting all the results in this section, we can claim that the derived tracking controller satisfies the control objective **(O1)**. Please notice that the final and complete computational algorithm related to the tracking controller is provided in Section 4.3.3 where it is denoted as **ST-MPC-i**.

4.3.2 Traffic Manager (TM) and Collision Avoidance

In this subsection, the traffic manager logic and the collision avoidance strategy solving the control objective **(O2)** are presented.

First, it is important to clarify which exchange of data is assumed between the local vehicles' controllers and the **TM**. This allows us to understand which information the **TM** can leverage to avoid collisions.

Data exchange over time:

- At $t = 0$: each i -th vehicle transmits to **TM** the computed family of robust one-step controllable sets centered in the first waypoint $r_i(0)$, $\{\mathcal{T}_i^l(r_i(0))\}_{l=0}^{N_i}$.
- At $t \geq 0$:

Each i -th vehicle sends to **TM**:

- The current set-membership index $l_i(t)$ (see *(On-1)*).
- The waypoint \bar{r}_i , where $\bar{r}_i = r_i(k_i + 1)$ (next waypoint) if the i -th UV is in a terminal region, $\bar{r}_i = r_i(k_i)$ (current waypoint), otherwise. Hereafter, we denote with $\mathcal{I}_{sw}(t) \subseteq \mathcal{I}$, the set of UVs making request to switch waypoint at time t .

TM sends to each i -th vehicle a binary variable which values are “Stop” or “Go”.

The next proposition states the fundamental set-theoretic condition under which a

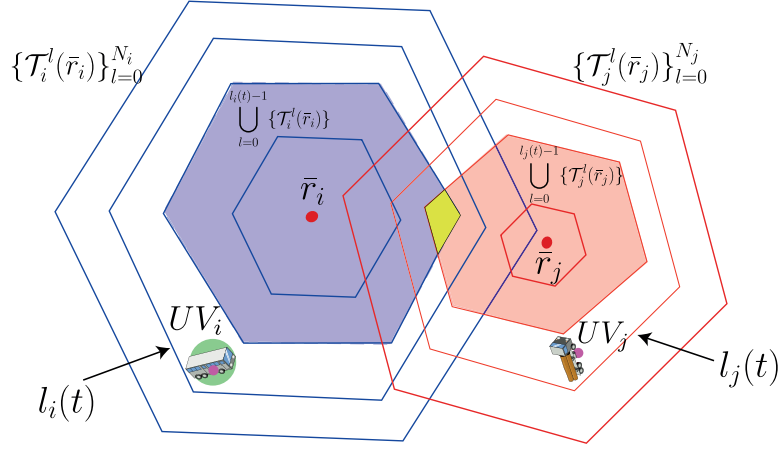


Figure 4.3.3: Possibility of collision between UV_i and UV_j . The possibility of collision is represented by the non-empty intersection (yellow area) between $\bigcup_{l=0}^{l_i(t)-1} \{\mathcal{T}_i^l(\bar{r}_i)\}$ (purple region) and $\bigcup_{l=0}^{l_j(t)-1} \{\mathcal{T}_j^l(\bar{r}_j)\}$ (pink region), see condition (61).

collision between two UVs might happen. Please refer to Fig. 4.3.3 for a graphical illustration.

Proposition 4. *Let's consider two UVs, namely UV_i and UV_j modeled as (1)-(2). Let $\{\mathcal{T}_i^l(\bar{r}_i)\}_{l=0}^{N_i}$ and $\{\mathcal{T}_j^l(\bar{r}_j)\}_{l=0}^{N_j}$ be the families of one-step controllable sets currently used by the ST-MPC controllers to track the waypoints \bar{r}_i and \bar{r}_j , respectively. If $l_i(t)$ and $l_j(t)$ are the set-membership indices at t , then a necessary condition for the existence of collisions at $t + 1$ is:*

$$C_{\bar{r}_i \bar{r}_j}(l_i(t), l_j(t)) := \bigcup_{l=0}^{\max(l_i(t)-1, 0)} \{\mathcal{T}_i^l(\bar{r}_i)\} \cap \bigcup_{l=0}^{\max(l_j(t)-1, 0)} \{\mathcal{T}_j^l(\bar{r}_j)\} \neq \emptyset \quad (61)$$

Proof. According to the ST-MPC online algorithm (see Steps (On-1)-(On-2)), the one-step evolution of each vehicle is confined within a set which set-membership index is less or equal to the current one. In particular, if UV_i is currently outside of the terminal region ($l_i(t) > 0$), then $l_i(t+1) < l_i(t)$, otherwise $l_i(t+1) = l_i(t)$. The same arguments apply to UV_j . As a consequence, condition (61) represents a necessary but not sufficient condition for collisions at the next time instant. \square

Corollary 1. *If the waypoints \bar{r}_i and \bar{r}_j are kept constant, the vehicle's state trajectories*

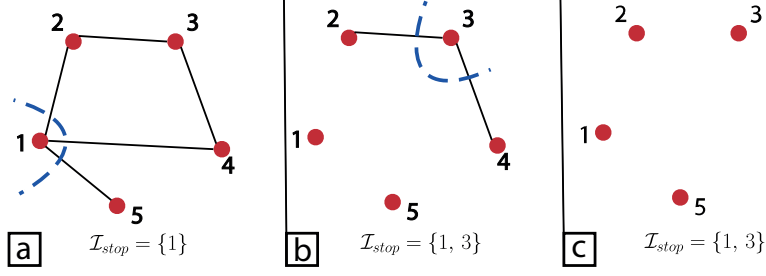


Figure 4.3.4: The subplot (a) shows the starting connectivity graph where the node $\bar{i} = 1$ is selected to be stopped according to the procedure (P1)-(P3) and condition (63). Subplot (b) shows that in the second iteration of (P1)-(P3), the node $\bar{i} = 3$ is stopped. Finally, subplot (c), shows the final disconnected graph that guarantees absence of collisions.

$x_i(t)$ and $x_j(t)$ are UUB in $\bigcup_{l=0}^{l_i(t)} \{\mathcal{T}_i^l(\bar{r}_i)\}$ and $\bigcup_{l=0}^{l_j(t)} \{\mathcal{T}_j^l(\bar{r}_j)\}$, respectively. As a consequence, if no collisions are predicted at \bar{t} , then no collisions can occur for any $t > \bar{t}$.

□

Given the result in *Proposition 4*, we want to design a conservative but effective traffic manager capable of ensuring that, for any pair (i, j) of UVs in \mathcal{I} , the potential collision condition (61) is never reached. To this end, first, a connectivity graph modeling all the possible intersections is built, and then a collision avoidance strategy capable of minimizing the number of vehicles to be stopped is illustrated.

For feasibility reasons, we assume that at $t = 0$ the condition (61), \forall pair (i, j) in \mathcal{I} , is not satisfied (no initial collisions). Therefore until no vehicle make a request to update the current waypoints, namely $r_i(k_i)$, $\forall i$, no collisions are possible (see *Corollary 1*). As soon as the first vehicle make the request to switch waypoint (i.e. the vehicle has reached the current terminal region), a connectivity graph, modeling potential collisions, i.e. $\mathcal{G}(t) = (\mathcal{V}, \mathcal{E}(t))$, is built as follows:

- $\mathcal{V} = \mathcal{I}$

-

$$e_{ij}(t) = \begin{cases} 1 & \text{if } i \in \mathcal{I}_{sw} \text{ and } \mathcal{C}_{\bar{r}_i \bar{r}_j}(l_i(t), l_j(t)) \neq \emptyset \\ 0 & \text{otherwise} \end{cases} \quad (62)$$

where $\bar{r}_p = r_p(k_p + 1)$ if $p \in \mathcal{I}_{sw}$, $\bar{r}_p = r_p(k_p)$ otherwise, $p = i, j$.

If at the time t , $\exists e_{ij}(t) \neq 0$, a collision avoidance strategy must be activated. In the sequel, we denote with $\mathcal{I}_{stop} \subseteq \mathcal{I}$ the set of vehicles that need to be stopped. It is important to remark that all the UV_i s making a switching request, $i \in \mathcal{I}_{sw}$, are already within RCI regions, i.e. $x_i(t) \in \mathcal{T}_i^0(r_i(k_i))$. Therefore, if needed, they can be stopped for an indefinitely long time period without causing collisions (see *Corollary 1*). Moreover, UV_i not making any request of waypoint switch cannot be stopped (they are not in a terminal RCI region). In order to stop the minimum number of UVs, the following procedure is applied:

(P1) Find the vehicle $\bar{i} \in \mathcal{I}_{sw}$ with the highest degree, i.e.

$$\bar{i} = \arg \max_{i \in \mathcal{I}_{sw}} \Delta[\mathcal{G}] \quad (63)$$

(P2) Add \bar{i} to \mathcal{I}_{stop} and set to zero all the edges connected to the node \bar{i} , i.e. $e_{\bar{i}j} = 0$
 $\forall j \in \mathcal{I}$

(P3) If $\exists e_{ij}(t) \in \mathcal{E}(t) : e_{ij}(t) \neq 0$, goto Step (P1)

For the sake of clarity, we explain the rationale behind the above algorithm by referring to Fig. 4.3.4. Let's consider a set of 5 vehicles, e.g. $\mathcal{I} = \{1, \dots, 5\}$ where UV_1 , UV_2 and UV_3 request a waypoint switch, i.e. $\mathcal{I}_{sw} = \{1, 2, 3\}$. The connectivity graph \mathcal{G} is the one shown in Fig. 4.3.4.a. The described (P1)-(P3) algorithm searches and stops the vehicle with the highest degree. The latter ensures that at each iteration, we remove the vehicle with the greatest number of possible collisions. In the first iteration, according to (63), the vehicle UV_1 is stopped and the edges e_{12} , e_{14} and e_{15} are removed (such collisions are not possible anymore). The resulting connectivity graph is shown in Fig. 4.3.4.b from which the second iteration starts and stops UV_3 . By removing the edges connected to UV_3 , i.e. e_{32} and e_{34} , the final disconnected graph in Fig. 4.3.4.c is obtained where no collisions are possible, and the (P1)-(P3) procedure is ended. Finally, the outcome is the set \mathcal{I}_{stop}

of vehicles that need to be stopped in the current terminal region, which in the specific example are $\mathcal{I}_{stop} = \{1, 3\}$.

4.3.3 Computation Algorithms

This section first summarizes all the above developments in two computation algorithms describing the logic of the local ST-MPC controllers and Traffic Manager. Then, a final concluding proposition is given to prove that the proposed control architecture ensures the absence of collisions regardless of the UVs reference trajectories (objective **(O2)**).

Traffic Manager (TM)

Input:

- At $t = 0$: $\{\mathcal{T}_i^l(r_i(0))\}_{l=0}^{N_i}, \forall i \in \mathcal{I}$;
- $\forall t : \mathcal{I}_{sw}, l_i(t), \bar{r}_i \forall i \in \mathcal{I}$

Output: “{Go, Stop}” for each $i \in \mathcal{I}$

$-\forall t :$

- 1: **if** $\mathcal{I}_{sw} = \emptyset$ **then** $\mathcal{I}_{stop} = \emptyset$
 - 2: **else**
 - 3: Build $\mathcal{G}(t) = (\mathcal{V}(t), \mathcal{E}(t))$ as in (62)
 - 4: **if** $\exists e_{ij}(t) \neq 0$ **then**
 - 5: Compute \mathcal{I}_{stop} by using (P1)-(P3)
 - 6: **else** $\mathcal{I}_{stop} = \emptyset$
 - 7: **end if**
 - 8: **end if**
 - 9: $\forall i \in \mathcal{I}$, if $i \in \mathcal{I}_{stop}$, send “Stop”, otherwise send “Go”
-

Set-Theoretic MPC i (**ST-MPC-i**)

Input: Off-line computations: $\forall i : \{\mathcal{T}_i^l(r_i(0))\}_{l=0}^{N_i}$, see (54)-(55)

Output: $u_i(t)$

$-\forall t :$

- 1: Use (56) to find the smallest set index $l_i(t)$ containing $x_i(t)$
 - 2: **if** $l_i(t) == 0$ **then**
 - 3: $\bar{r}_i \leftarrow r_i(k_i + 1)$ \triangleright attempt to switch waypoint
 - 4: **else**
 - 5: $\bar{r}_i \leftarrow r_i(k_i)$ \triangleright keep the same waypoint
 - 6: **end if**
 - 7: Send to **TM**: $l_i(t), \bar{r}_i$
 - 8: **if** $l_i(t) == 0$ & **TM** == “Go” **then** \triangleright switch authorized
 - 9: $r_i(k_i) \leftarrow r_i(k_i + 1), k_i \leftarrow k_i + 1;$
 - 10: Update $l_i(t)$ by using (56)
 - 11: **end if**
 - 12: **if** $l_i(t) == 0$ **then** $u_i(t) = K_i^0(x_i(t) - x_{r_i}^{eq}(k_i))$
 - 13: **else** Find $u_i(t)$ by solving opt. (57)
 - 14: **end if**
 - 15: Apply $u_i(t), t \leftarrow t + 1$ and goto Step 1
-

Remark 8. *The computational complexity of the proposed **TM** algorithm is mainly related to the construction of $\mathcal{G}(t)$ in Step 2. In particular, to test if between two vehicles i and j there is a collision possibility (i.e., $e_{ij}(t) = 1$), then a set-membership test must be performed. Assuming a polyhedral representation for the robust one-step controllable sets \mathcal{T}_i^l , each test requires the solution of a simple linear programming (LP) optimization*

problem solvable in polynomial time. Therefore, to completely build $\mathcal{G}(t)$, the number of LP problems that must be solved is equal to $|\mathcal{I}_{sw}(t)|(S - 1)$ where $|\mathcal{I}_{sw}|$ is the number of vehicles making a waypoint switch request at the time t and S is the total number of vehicles. On the other hand, the local **ST-MPC-i** is mainly related to the solution of the QP optimization problem defined in (57). Therefore, contrary to the existing DMPC solutions, the proposed approach does not require inter-vehicles communications and non-convex optimizations. As an example, at each iteration, the distributed approach in [62] requires the computation of S MILPs while the proposed solution requires $S(S - 1)$ LPs (worst-case) and 1 QP per vehicle.

Task Solved	Proposed Sol.	[62]
Collision Avoidance	$S(S - 1)$ LPs	(S) MILPs
Reference Tracking	(1) QP per vehicle	

Proposition 5. Let's consider a set \mathcal{I} of UVs modeled as in (1)-(2) where each i -th UV is equipped with the **ST-MPC-i** local controller and the vehicles waypoint switches are coordinated by a centralized traffic manager which logic is described by the **TM** algorithm. If the UVs start from a feasible collision-free initial condition, i.e.

$$\exists l_i(0) \geq 0 : x_i(0) \in \bigcup_{l=0}^{l_i(0)} \mathcal{T}_i^l(r_i(0)), \quad \forall i \in \mathcal{I} \quad (64)$$

$$\bigcup_{l=0}^{l_i(0)} \mathcal{T}_i^l(r_i(0)) \cap \bigcup_{l=0}^{l_j(0)} \mathcal{T}_j^l(r_j(0)) = \emptyset, \quad \forall (i, j), \quad i \neq j, \quad i, j \in \mathcal{I} \quad (65)$$

then, **TM** guarantees the absence of collisions, i.e. $\|p_i(t) - p_j(t)\|_2 > 0, \quad \forall t \in \mathbb{Z}_+, \quad \forall i, j \in \mathcal{I}, \quad i \neq j$ regardless of the UVs trajectories $\mathbf{r}_i, \forall i \in \mathcal{I}$.

Proof. If each i -th UV starts from a feasible collision-free initial condition, see (64)-(65), then **ST-MPC-i** controller is capable of steering each UV state trajectory within

the current terminal RCI region in a finite number of steps (see ST-MPC-i, Steps 12-15) where it can be confined for an arbitrarily long time interval. Moreover, according to the results in *Proposition 4* and *Corollary 1*, until no waypoint switch occurs, collisions among vehicles are not possible. In *Proposition 3* it has been proved that starting from a terminal region, e.g. $\mathcal{T}_i^0(r_i(k_i))$ waypoint switches $r_i(k_i) \rightarrow r_i(k_i + 1)$ are always feasible and preserve vehicle constraints (2). On the other hand, to avoid collisions among the vehicles, switches can be accomplished only if the collision avoidance condition (61) is preserved between any pair of vehicles. To this end, each vehicle, before switching, asks permission to the **TM** (see ST-MPC-i, Step 8) who collects all the requests. The **TM**, by building the connectivity graph (see TM, Step 3), checks if any of the requested waypoint switches do not preserve (61) (see TM, Step. 4). If collisions are detected, then the procedure (P1)-(P3) is activated (see TM, Steps. 5) to deny the waypoint switch to the minimum number of vehicles. The latter is sufficient to maintain the vehicles controllers' domain mutually disjointed, i.e.

$$\bigcup_{l=0}^{l_i(t)} \mathcal{T}_i^l(r_i(k_i)) \cap \bigcup_{l=0}^{l_j(t)} \mathcal{T}_j^l(r_j(k_j)) = \emptyset, \forall (i, j), i \neq j, i, j \in \mathcal{I}$$

and ensure absence of collisions, concluding the proof. \square

4.4 Simulation

In this section, the effectiveness of the proposed control architecture is testified by means of a simulation example involving five vehicles. The whole system has been emulated within the MATLAB environment and the MPT3 toolbox [79], which has been used to implement the **ST-MPC-i** and **TM** algorithms.

We consider a family of 5 UVs, $\mathcal{I} = \{1, \dots, 5\}$ whose dynamics are described by means of a double integrator model [83] which state space vector $x \in \mathbb{R}^4$ includes the positions (p^x, p^y) and velocities (v^x, v^y) . The input signals $u \in \mathbb{R}^2$ are the two accelerations

(a^x, a^y) and the discrete-time LTI system matrices (1), obtained by using a sampling time $T_s = 0.1$ sec, are:

$$A_i = \begin{bmatrix} 1 & 0 & 0.1 & 0 \\ 0 & 1 & 0 & 0.1 \\ 0 & 0 & 1 & 0 \\ 0 & 0 & 0 & 1 \end{bmatrix}, B_i = \begin{bmatrix} 0.005 & 0 \\ 0 & 0.005 \\ 0.1 & 0 \\ 0 & 0.1 \end{bmatrix}, \forall i \in \mathcal{I}$$

We assume that the vehicles are subject to the following state and input constraints and disturbances:

$$\begin{aligned} |u_1^x| \leq 20, |u_1^y| \leq 15, \quad |u_3^x| \leq 10, |u_3^y| \leq 12 \\ |u_5^x| \leq 25, |u_5^y| \leq 22 \end{aligned}$$

where, $|u_2^x| = |u_3^x|, |u_2^y| = |u_3^y|, |u_4^x| = |u_5^x|, |u_4^y| = |u_5^y|$ and,

$$\begin{aligned} \mathcal{D}_1 &= \{d \in \mathbb{R}^4 : -0.07 \leq d_i \leq 0.07, i = 1, \dots, 4\} \\ \mathcal{D}_2 &= \mathcal{D}_3 = \{d \in \mathbb{R}^4 : -0.08 \leq d_i \leq 0.08, i = 1, \dots, 4\} \\ \mathcal{D}_4 &= \mathcal{D}_5 = \{d \in \mathbb{R}^4 : -0.05 \leq d_i \leq 0.05, i = 1, \dots, 4\} \end{aligned}$$

It is worth noticing that the above bounds are not the same for all vehicles. This has been done to model the presence of vehicles with different performances and/or capabilities.

We assume that the vehicles' trajectories are uncoordinated and have possible intersection points. In particular, each vehicle's reference generator provides the waypoints $r_i(k_i)$ obtained from the following discrete functions

$$\begin{bmatrix} r_1(k)^T \\ r_2(k)^T \\ r_3(k)^T \\ r_4(k)^T \\ r_5(k)^T \end{bmatrix} = \begin{bmatrix} 10 \sin(0.09k) & 5k \\ 10 \sin(0.25k) & 5k \\ 10 \sin(-0.45k) & 5k \\ 10 \sin(-0.18k) & 5k \\ 10 \sin(-0.23k) & 5k \end{bmatrix} \quad (66)$$

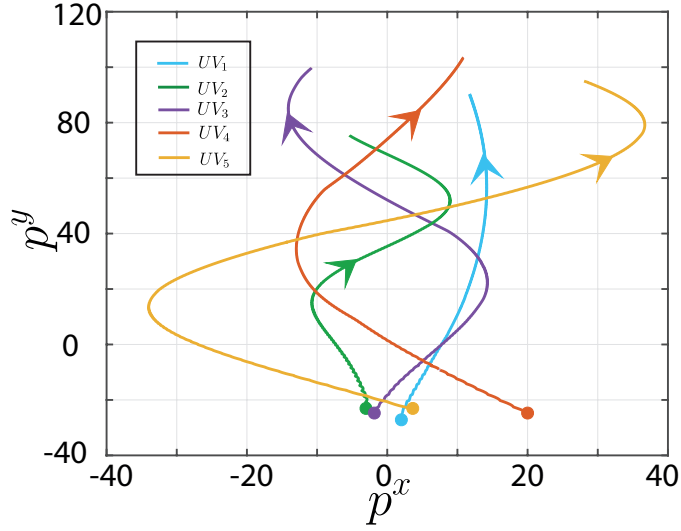


Figure 4.4.1: Vehicles' trajectories for $t \in [0, 100]s$

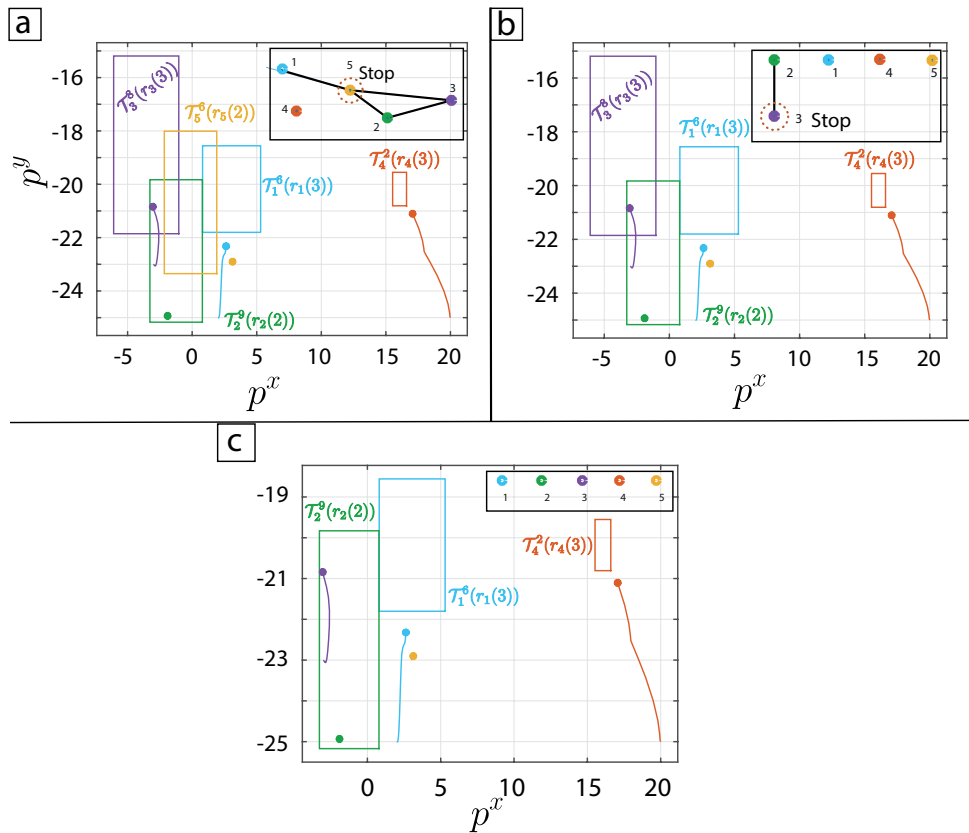


Figure 4.4.2: Potential collision at $t = 1.5s$. Subplot [a] shows the existing intersections between the families of one-step controllable sets and the corresponding connectivity graph $\mathcal{G}(1.5)$. Subplot [b] shows the remaining collisions when UV_5 is stopped. Subplot [c] shows the absence of collision when both UV_3 and UV_5 are stopped.

where the maximum distance $\delta_i, \forall i \in \mathcal{I}$ between two successive waypoints are: $\delta_1 = 2.56, \delta_2 = \delta_3 = 2.61, \delta_4 = \delta_5 = 3.89$, According to the proposed ST-MPC strategy, for each vehicle, a terminal controller and a family of RCI sets have been offline computed as prescribed in (54)-(55). The used LQ terminal controllers gain is

$$K_i^0 = \begin{bmatrix} -27.3037 & 0 & -7.6377 & 0 \\ 0 & -27.3037 & 0 & -7.6377 \end{bmatrix}, \forall i$$

On the other hand, to assure that the vehicles' controller domains satisfy the waypoint switching feasibility condition (59), the following families of robust controllable sets have been computed

$$\{\mathcal{T}_1^l\}_{l=0}^{20}, \{\mathcal{T}_{2,3}^l\}_{l=0}^{22}, \{\mathcal{T}_{4,5}^l\}_{l=0}^{23}$$

By assigning to each vehicle the following initial conditions

$$\begin{bmatrix} x_1(0)^T \\ x_2(0)^T \\ x_3(0)^T \\ x_4(0)^T \\ x_5(0)^T \end{bmatrix} = \begin{bmatrix} 2 & -25 & 0 & 0 \\ -2 & -20 & 0 & 0 \\ -3 & -23 & 0 & 0 \\ 20 & -25 & 0 & 0 \\ 3 & -23 & 0 & 0 \end{bmatrix}$$

the simulation results provided in Figs. 4.4.1-4.4.3 are obtained.

In Fig. 4.4.1, the vehicle's trajectories are depicted for the time interval $[0, 100]s$. The trajectories show how the vehicles' local **ST-MPC-i** controllers are able to track the switching waypoints (66) despite constraints and disturbances. Moreover, it is possible to notice that the obtained paths have potential collision points. Therefore, it is worth to investigate how the traffic manager actions are essential to avoid collisions. To better understand the **TM modus operandi**, we shall refer to Fig. 4.4.2 where the simulation has been paused at $t = 1.5s$. Specifically, at the considered screenshot, the vehicle's set membership scenario is the following:

$$x_1(1.5) \in \mathcal{T}_1^7(r_1(3)), \quad UV_2 \in \mathcal{T}_2^0(r_2(1))$$

$$x_3(1.5) \in \mathcal{T}_3^0(r_3(2)), \quad UV_4 \in \mathcal{T}_4^3(r_4(3))$$

$$x_5(1.5) \in \mathcal{T}_5^0(r_5(1))$$

The **TM**, first collects all the waypoint switch requests and set-membership indices. At $t = 1.5s$, UV_2, UV_3, UV_5 are within a terminal region (i.e. $l_2(1.5) = l_3(1.5) = l_5(1.5) = 0$) while UV_1, UV_4 are inside one-step controllable sets (i.e. $l_1(1.5) = 7$ and $l_4(1.5) = 3$). By construction, the waypoint switch feasibility condition (59) ensures that the vehicles in the terminal region also belong to the family of the one-step controllable set associated with the successive waypoint. In particular:

$$x_2(1.5) \in \mathcal{T}_2^{10}(r_2(2)), \quad x_3(1.5) \in \mathcal{T}_3^9(r_3(3)), \quad x_5(1.5) \in \mathcal{T}_5^7(r_5(2))$$

As a consequence, the set of vehicles candidate for a switch request is $\mathcal{I}_{sw} = \{2, 3, 5\}$.

Given the collected information, the **TM** builds the connectivity graph $\mathcal{G}(1.5)$ according to (62). In Fig. 4.4.2.a, the current vehicles' positions are shown with small colored circles and the rectangular areas (matched by color) represent the region where the one-step evolution (at $t = 1.6s$) of each agent will be confined, i.e.

$$\begin{aligned} x_1(1.6) &\in \bigcup_{l=0}^6 \mathcal{T}_1^l(r_1(3)), & x_2(1.6) &\in \bigcup_{l=0}^9 \mathcal{T}_2^l(r_2(2)), \\ x_3(1.6) &\in \bigcup_{l=0}^8 \mathcal{T}_3^l(r_3(3)), & x_4(1.6) &\in \bigcup_{l=0}^2 \mathcal{T}_4^l(r_4(3)), \\ x_5(1.6) &\in \bigcup_{l=0}^6 \mathcal{T}_5^l(r_5(2)) \end{aligned} \quad (67)$$

Since the constructed families of one-step controllable sets are nested, in Fig. 4.4.2, we show only the last sets, which are equivalent to the unions in (67). The connectivity graph shown in the top-right corner of Fig. 4.4.2.a. summarizes all the possible collisions between the regions in (67), see (61). The graph presents potential collisions among the agents 1, 2,

3 and 5. Therefore, according to the **TM** algorithm (see step 5) the (P1)-(P3) procedure is activated to avoid collisions by stopping the minimum number of vehicles among the ones making a waypoint switch request. First, the UV_5 (the node with the highest degree) is stopped and added to \mathcal{I}_{stop} . As a consequence, all the edges connected to UV_5 are also removed. The resulting novel connectivity graph and remaining intersections are shown in Fig. 4.4.2.b. Since a collision is still possible between UV_2 and UV_3 , i.e.

$$\mathcal{T}_2^9(r_2(2)) \cap \mathcal{T}_3^8(r_3(3)) \neq \emptyset$$

a second iteration of (P1)-(P3) is executed and the vehicle UV_3 is added to \mathcal{I}_{stop} . At this point, with

$$\mathcal{I}_{stop} = \{3, 5\} \tag{68}$$

the completely disconnected graph in Fig. 4.4.2.c results where no collisions are possible. Therefore, the **TM** operations are concluded: UV_3 and UV_5 are stopped while UV_2 is allowed to switch waypoint.

In Fig. 4.4.3, the vehicles set-membership index signal is shown for the time interval $[0, 25]s$, (the time interval has been shortened to improve the figure's readability). The latter allows us to better clarify the stop and go commands received by each vehicle according to the **TM** operations previously described. In the absence of collisions, the signals $l_i(t)$, by construction, have a reverse sawtooth shape. The wave ramps downward while the vehicles move within the family of computed one-step controllable sets, and sharply rises when a waypoint switch occurs. On the other hand, when the signal $l_i(t)$ holds constant for more than one sampling time, then it means that the vehicle i has received a STOP command. It is worth noticing in Fig. 4.4.3 that, according to the developed theory, a STOP signal can be received only by the vehicles making switch request, i.e. from the vehicles within a terminal region ($l_i(t) = 0$). As an example, in the previously described potential collision happening at $t = 1.5s$, the **TM** imposes a stop

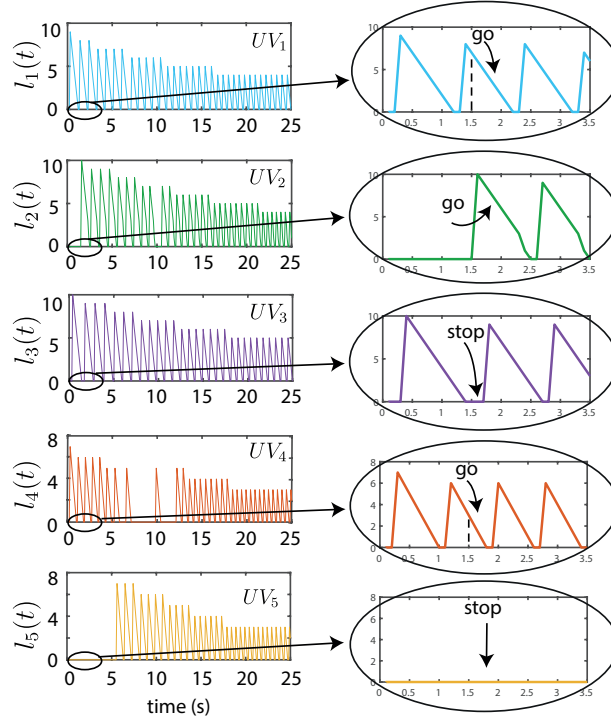


Figure 4.4.3: Vehicles’ set membership indices in the time interval $[0 - 25]s$ (left side) and zoom-in in the time interval $[0 - 3.5]s$ (right side).

on two of the three vehicles making a switch request, i.e. UV_3 and UV_5 (see (68)). As a consequence in the zoom-in subplot in Fig. 4.4.3, it is possible to appreciate what follows: the signal $l_3(1.5)$ and $l_5(1.5)$ stays constant to zero, meaning that the waypoint switch has been denied for UV_3 and UV_5 ; the index l_2 jumps from 0 to $l_2 = 10$, testifying that the waypoint switch has been granted to UV_2 ; the signals $l_1(t)$ and $l_4(t)$ keep decreasing showing that both UV_1 and UV_4 keep moving closer to the current waypoint.

4.5 Conclusion

In this chapter, we have presented a novel solution to deal with the collision avoidance problem for heterogeneous constrained vehicles moving in a shared environment. We have proposed a control architecture where each vehicle is equipped with a local set-theoretic MPC tracking controller and a centralized traffic manager, exploiting simple set-membership arguments, guarantees absence of collisions. We have proved that the

proposed solution is sufficient to guarantee collision avoidance despite vehicle constraints, disturbance realization and desired vehicle's trajectories. The latter has been achieved by assuring that during the waypoint switches a specific set-theoretic absence of collisions condition is a system invariant. Moreover, by modeling the potential collisions as a connectivity graph, we have proposed a strategy that minimizes, at each time, the number of vehicles that need to be stopped. Finally, we have shown the effectiveness and potential of the proposed technology by means of a simulation campaign involving five vehicles.

Chapter 5

Conclusion

In this thesis, we have extended the set-theoretic MPC paradigm to deal with two different control problems, namely transient stability in smart grid systems (regulation) and collision-free reference tracking of multi unmanned vehicles (reference tracking).

In the transient stability problem, a controller consisting of two feedback actions is proposed, where the first partially compensates the effect of nonlinear dynamical coupling among generators, and the second exploits set-theoretic arguments to robustly guarantee transient stability despite non perfect decoupling, disturbances and physical limitations of the fast acting energy storage system. Moreover, the robust nature of the proposed controller is formally proved and it is shown that a worst-case time to transient stability recovery can be formally assured. To better highlight the properties of the controller, its performance has been contrasted with the recent solution given in [34] by means of a solid simulation example.

In the multi-UV system, a control architecture has been presented where each vehicle is equipped with a local set-theoretic MPC tracking controller and a centralized traffic manager that guarantees optimal collision avoidance by exploiting simple set-membership arguments and resorting to graph connectivity theory. It is considered that each vehicle is equipped with a reference generator module where the vehicles' reference trajectories might not be coordinated. Differently from the discussed state-of-the-art, it is proved

that the solution here presented is capable of managing heterogeneous constrained MUVs subject to bounded disturbances, and collision-free movements are, by design, ensured regardless of the trajectory followed by the vehicles. Simulation results, conducted on a system of five vehicles, has been provided to provide tangible evidence of the features of the proposed framework.

In both applications, the resulting control schemes have been characterized for their peculiar capability of reducing the typical computation burden of robust MPC controllers. In particular, the latter has been achieved by moving most of the algorithm into an off-line phase. In the online phase, the control action computation cost is modest and it requires the solution of a simple convex optimization problem.

Bibliography

- [1] J. M. Maciejowski, *Predictive control: with constraints*. Pearson education, 2002.
- [2] C. E. Garcia, D. M. Prett, and M. Morari, “Model predictive control: theory and practice—a survey,” *Automatica*, vol. 25, no. 3, pp. 335–348, 1989.
- [3] M. Kothare, V. Balakrishnan, and M. Morari, “Robust constrained model predictive control using linear matrix inequalities,” *Automatica*, vol. 32, no. 10, pp. 1361–1379, 1996.
- [4] P. O. Scokaert and D. Mayne, “Min-max feedback model predictive control for constrained linear systems,” *IEEE Transactions on Automatic control*, vol. 43, no. 8, pp. 1136–1142, 1998.
- [5] K. R. Muske and T. A. Badgwell, “Disturbance modeling for offset-free linear model predictive control,” *Journal of Process Control*, vol. 12, no. 5, pp. 617–632, 2002.
- [6] J. V. Frasch, A. Gray, M. Zanon, H. J. Ferreau, S. Sager, F. Borrelli, and M. Diehl, “An auto-generated nonlinear mpc algorithm for real-time obstacle avoidance of ground vehicles,” in *IEEE European Control Conference (ECC)*, 2013, pp. 4136–4141.
- [7] P. Falcone, F. Borrelli, J. Asgari, H. E. Tseng, and D. Hrovat, “Predictive active steering control for autonomous vehicle systems,” *IEEE Transactions on control systems technology*, vol. 15, no. 3, pp. 566–580, 2007.

- [8] S. Di Cairano, D. Bernardini, A. Bemporad, and I. V. Kolmanovsky, “Stochastic mpc with learning for driver-predictive vehicle control and its application to hev energy management,” *IEEE Transactions on Control Systems Technology*, vol. 22, no. 3, pp. 1018–1031, 2013.
- [9] A. Richards and J. How, “Mixed-integer programming for control,” in *IEEE American Control Conference (ACC)*, 2005, pp. 2676–2683.
- [10] R. R. Negenborn and J. M. Maestre, “Distributed model predictive control: An overview and roadmap of future research opportunities,” *IEEE Control Systems Magazine*, vol. 34, no. 4, pp. 87–97, 2014.
- [11] A. N. Venkat, I. A. Hiskens, J. B. Rawlings, and S. J. Wright, “Distributed mpc strategies with application to power system automatic generation control,” *IEEE Transactions on control systems technology*, vol. 16, no. 6, pp. 1192–1206, 2008.
- [12] A. Alessio and A. Bemporad, “A survey on explicit model predictive control,” in *Nonlinear model predictive control*. Springer, 2009, pp. 345–369.
- [13] P. Campo and M. Morari, “Robust model predictive control,” in *IEEE American control conference*, 1987, pp. 1021–1026.
- [14] A. Bemporad and M. Morari, “Robust model predictive control: A survey,” in *Robustness in identification and control*. Springer, 1999, pp. 207–226.
- [15] M. E. Villanueva, R. Quirynen, M. Diehl, B. Chachuat, and B. Houska, “Robust mpc via min–max differential inequalities,” *Automatica*, vol. 77, pp. 311–321, 2017.
- [16] Z. Q. Zheng and M. Morari, “Robust stability of constrained model predictive control,” in *IEEE American Control Conference (ACC)*, 1993, pp. 379–383.

- [17] J. Allwright and G. Papavasiliou, “On linear programming and robust model-predictive control using impulse-responses,” *Systems & Control Letters*, vol. 18, no. 2, pp. 159–164, 1992.
- [18] M. Cannon and B. Kouvaritakis, “Optimizing prediction dynamics for robust mpc,” *IEEE Transactions on Automatic Control*, vol. 50, no. 11, pp. 1892–1897, 2005.
- [19] P. Gutman and M. Cwikel, “Admissible sets and feedback control for discrete-time linear dynamical systems with bounded controls and states,” *IEEE Transactions on Automatic Control*, vol. 31, no. 4, pp. 373–376, 1986.
- [20] A. Bemporad, M. Morari, V. Dua, and E. Pistikopoulos, “The explicit linear quadratic regulator for constrained systems,” *Automatica*, vol. 38, no. 1, pp. 3–20, 2002.
- [21] F. Borrelli, *Constrained optimal control of linear and hybrid systems*. Springer, 2003, vol. 290.
- [22] E. Kerrigan and J. M. Maciejowski, “Feedback min-max model predictive control using a single linear program: robust stability and the explicit solution,” *International Journal of Robust and Nonlinear Control: IFAC-Affiliated Journal*, vol. 14, no. 4, pp. 395–413, 2004.
- [23] Y. Wang and S. Boyd, “Fast model predictive control using online optimization,” *IEEE Transactions on control systems technology*, vol. 18, no. 2, pp. 267–278, 2009.
- [24] F. Blanchini and S. Miani, *Set-theoretic methods in control*. Springer, 2008.
- [25] D. Angeli, A. Casavola, G. Franzè, and E. Mosca, “An ellipsoidal off-line mpc scheme for uncertain polytopic discrete-time systems,” *Automatica*, vol. 44, no. 12, pp. 3113–3119, 2008.

- [26] W. Lucia, D. Famularo, and G. Franzè, “A set-theoretic reconfiguration feedback control scheme against simultaneous stuck actuators,” *IEEE Trans. on Automatic Control*, vol. 63, no. 8, pp. 2558–2565, 2018.
- [27] M. Zeilinger, D. M. Raimondo, A. Domahidi, M. Morari, and C. Jones, “On real-time robust model predictive control,” *Automatica*, vol. 50, no. 3, pp. 683–694, 2014.
- [28] W. Wang and Z. Lu, “Cyber security in the smart grid: Survey and challenges,” *Computer Networks*, vol. 57, no. 5, pp. 1344–1371, 2013.
- [29] Y. Yan, Y. Qian, H. Sharif, and D. Tipper, “A survey on smart grid communication infrastructures: Motivations, requirements and challenges,” *IEEE communications surveys & tutorials*, vol. 15, no. 1, pp. 5–20, 2013.
- [30] D. Wu, K. Chau, C. Liu, S. Gao, and F. Li, “Transient stability analysis of smes for smart grid with vehicle-to-grid operation,” *IEEE Trans. on Applied Superconductivity*, vol. 22, no. 3, pp. 5 701 105–5 701 105, 2012.
- [31] P. Anderson, A. Fouad, and H. Happ, “Power system control and stability,” *IEEE Transactions on Systems, Man, and Cybernetics*, vol. 9, no. 2, pp. 103–103, 1979.
- [32] N. Ratmarao and D. K. Reitan, “Improvement of power system transient stability using optimal control: bang-bang control of reactance,” *IEEE Transactions on Power Apparatus and Systems*, vol. 89, no. 5, pp. 975–984, 1970.
- [33] M. Ayar, S. Obuz, R. D. Trevizan, A. S. Bretas, and H. A. Latchman, “A distributed control approach for enhancing smart grid transient stability and resilience,” *IEEE Transactions on Smart Grid*, vol. 8, no. 6, pp. 3035–3044, 2017.
- [34] A. Farraj, E. Hammad, and D. Kundur, “A cyber-enabled stabilizing control scheme for resilient smart grid systems,” *IEEE Transactions on Smart Grid*, vol. 7, no. 4, pp. 1856–1865, 2016.

- [35] A. Farraj., E. Hammad, and D. Kundur, “A cyber-physical control framework for transient stability in smart grids,” *IEEE Transactions on Smart Grid*, vol. 9, no. 2, pp. 1205–1215, 2018.
- [36] M. Ayar, R. D. Trevizan, S. Obuz *et al.*, “Cyber-physical robust control framework for enhancing transient stability of smart grids,” *IET Cyber-Physical Systems: Theory & Applications*, vol. 2, no. 4, pp. 198–206, 2017.
- [37] A. Benzaouia, F. Mesquine, and M. Benhayoun, *Saturated control of linear systems*. Springer, 2018.
- [38] S. Tarbouriech, G. Garcia, and A. H. Glattfelder, *Advanced strategies in control systems with input and output constraints*. Springer, 2007, vol. 346.
- [39] S. Raković, “Robust model-predictive control,” *Encyclopedia of Systems and Control*, pp. 1225–1233, 2015.
- [40] Y. Cao, W. Yu, W. Ren, and G. Chen, “An overview of recent progress in the study of distributed multi-agent coordination,” *IEEE Transactions on Industrial informatics*, vol. 9, no. 1, pp. 427–438, 2013.
- [41] J.-C. Latombe, *Robot motion planning*. Springer Science & Business Media, 2012, vol. 124.
- [42] B. Paden, M. Čáp, S. Z. Yong, and E. Yershov, D.and Frazzoli, “A survey of motion planning and control techniques for self-driving urban vehicles,” *IEEE Transactions on intelligent vehicles*, vol. 1, no. 1, pp. 33–55, 2016.
- [43] J. Wit, C. D. Crane III, and D. Armstrong, “Autonomous ground vehicle path tracking,” *Journal of Robotic Systems*, vol. 21, no. 8, pp. 439–449, 2004.

- [44] A. P. Aguiar and J. P. Hespanha, “Trajectory-tracking and path-following of underactuated autonomous vehicles with parametric modeling uncertainty,” *IEEE Transactions on Automatic Control*, vol. 52, no. 8, pp. 1362–1379, 2007.
- [45] X. Dong, B. Yu, Z. Shi, and Y. Zhong, “Time-varying formation control for unmanned aerial vehicles: Theories and applications,” *IEEE Transactions on Control Systems Technology*, vol. 23, no. 1, pp. 340–348, 2015.
- [46] K. L. Fetzner, S. Nersesov, and H. Ashrafiuon, “Sliding mode control of underactuated vehicles in three-dimensional space,” in *IEEE American Control Conference (ACC)*, 2018, pp. 5344–5349.
- [47] M. Egerstedt and X. Hu, “Formation constrained multi-agent control,” *IEEE Transactions on Robotics and Automation*, vol. 17, no. 6, pp. 947–951, 2001.
- [48] S. Mastellone, D. M. Stipanović, C. R. Graunke, K. A. Intlekofer, and M. W. Spong, “Formation control and collision avoidance for multi-agent non-holonomic systems: Theory and experiments,” *International Journal of Robotics Research*, vol. 27, no. 1, pp. 107–126, 2008.
- [49] L. Wang, A. D. Ames, and M. Egerstedt, “Safety barrier certificates for collisions-free multirobot systems,” *IEEE Transactions on Robotics*, vol. 33, no. 3, pp. 661–674, 2017.
- [50] J. Minguez, F. Lamiroux, and J.-P. Laumond, “Motion planning and obstacle avoidance,” in *Springer handbook of robotics*. Springer, 2008, pp. 827–852.
- [51] Y. Kodama and K. Nakatani, “Collision avoidance system,” 2018, - U.S. Patent No. 5,529,138.
- [52] L. Fedele, G. and D’Alfonso, “A model for swarm formation with reference tracking,” in *IEEE Conference on Decision and Control (CDC)*. IEEE, 2017, pp. 381–386.

- [53] H. M. Guzey, T. Dierks, and S. Jagannathan, “Hybrid consensus-based formation control of agents with second order dynamics.” in *IEEE American Control Conference (ACC)*, 2015, pp. 4386–4391.
- [54] P. Ogren, E. Fiorelli, and N. E. Leonard, “Cooperative control of mobile sensor networks: Adaptive gradient climbing in a distributed environment,” *IEEE Transactions on Automatic control*, vol. 49, no. 8, pp. 1292–1302, 2004.
- [55] J. A. Fax and R. M. Murray, “Information flow and cooperative control of vehicle formations,” *IEEE Transactions on Automatic Control*, vol. 49, no. 9, pp. 1465–1476, 2004.
- [56] H. Liu, X. Dong, F. L. Lewis, Y. Wan, and K. P. Valavanis, “Robust formation control for multiple quadrotors subject to nonlinear dynamics and disturbances,” in *IEEE International Conference on Control and Automation (ICCA)*, 2018, pp. 58–62.
- [57] H. Du, W. Zhu, G. Wen, Z. Duan, and J. Lü, “Distributed formation control of multiple quadrotor aircraft based on nonsmooth consensus algorithms,” *IEEE Transactions on cybernetics*, no. 99, pp. 1–12, 2017.
- [58] X. Wang, M. Kloetzer, C. Mahulea, and M. Silva, “Collision avoidance of mobile robots by using initial time delays,” in *IEEE Conference on Decision and Control (CDC)*, 2015, pp. 324–329.
- [59] M. Chen, J. C. Shih, and C. J. Tomlin, “Multi-vehicle collision avoidance via hamilton-jacobi reachability and mixed integer programming,” in *IEEE Conference on Decision and Control (CDC)*, 2016, pp. 1695–1700.
- [60] W. B. Dunbar and D. S. Caveney, “Distributed receding horizon control of vehicle platoons: Stability and string stability,” *IEEE Transactions on Automatic Control*, vol. 57, no. 3, pp. 620–633, 2012.

- [61] H. Fukushima, K. Kon, and F. Matsuno, “Model predictive formation control using branch-and-bound compatible with collision avoidance problems,” *IEEE Transactions on Robotics*, vol. 29, no. 5, pp. 1308–1317, 2013.
- [62] A. Richards and J. How, “Decentralized model predictive control of cooperating uavs,” in *IEEE Conference on Decision and Control (CDC)*, vol. 4, 2004, pp. 4286–4291.
- [63] K.-D. Kim and P. R. Kumar, “An mpc-based approach to provable system-wide safety and liveness of autonomous ground traffic.” *IEEE Transactions on Automatic Control*, vol. 59, no. 12, pp. 3341–3356, 2014.
- [64] W. Lucia, K. Gheitasi, and M. Bagherzadeh, “A low computationally demanding model predictive control strategy for robust transient stability in smart grid,” in *IEEE Conference on Decision and Control (CDC)*, 2018, pp. 6013–6018.
- [65] M. Bagherzadeh and W. Lucia, “Multi-vehicle reference tracking with guaranteed collision avoidance,” in *IEEE European Control Conference (ECC)*, 2019, pp. 1574–1579.
- [66] M. Bagherzadeh. and W. Lucia, “A set-theoretic model predictive control approach for transient stability in smart grid,” *IET Control Theory & Applications*, vol. 14, no. 5, pp. 700–707, 2019.
- [67] W. Brogan, *Modern control theory*. Pearson education india, 1991.
- [68] S. V. Rakovic, E. C. Kerrigan, K. I. Kouramas *et al.*, “Invariant approximations of the minimal robust positively invariant set,” *IEEE Transactions on Automatic Control*, vol. 50, no. 3, pp. 406–410, 2005.
- [69] C. Canizares, T. Fernandes, E. Geraldi Jr *et al.*, “Benchmark systems for small signal stability analysis and control,” <http://resourcecenter.ieee-pes.org/pes/product/technical-reports/PESTR18>, no. PES-TR, 2015.

- [70] J. Chapman, M. Ilic, C. King *et al.*, “Stabilizing a multimachine power system via decentralized feedback linearizing excitation control,” *IEEE Transactions on Power Systems*, vol. 8, no. 3, pp. 830–839, 1993.
- [71] Q. Hu, D. Fooladivanda, Y. H. Chang *et al.*, “Secure state estimation and control for cyber security of the nonlinear power systems,” *IEEE Transactions on Control of Network Systems*, vol. 5, no. 3, pp. 1310–1321, 2017.
- [72] H. D. Chiang, F. F. Wu, and P. Varaiya, “Foundations of direct methods for power system transient stability analysis,” *IEEE Transactions on Circuits and systems*, vol. 34, no. 2, pp. 160–173, 1987.
- [73] H. D. Chiang, F. Wu, and P. Varaiya, “A bcu method for direct analysis of power system transient stability,” *IEEE Transactions on Power Systems*, vol. 9, no. 3, pp. 1194–1208, 1994.
- [74] A. Bose, “Smart transmission grid applications and their supporting infrastructure,” *IEEE Transactions on Smart Grid*, vol. 1, no. 1, pp. 11–19, 2010.
- [75] A. Isidori, *Nonlinear control systems*. Springer Science & Business Media, 2013.
- [76] E. Hammad, A. Farraj, and D. Kundur, “On effective virtual inertia of storage-based distributed control for transient stability,” *IEEE Transactions on Smart Grid*, vol. 10, no. 1, pp. 327–336, 2017.
- [77] M. A. Mahmud, H. R. Pota, M. Aldeen *et al.*, “Partial feedback linearizing excitation controller for multimachine power systems to improve transient stability,” *IEEE Transactions on Power systems*, vol. 29, no. 2, pp. 561–571, 2013.
- [78] Y. Guo, D. J. Hill, and Y. Wang, “Global transient stability and voltage regulation for power systems,” *IEEE transactions on power systems*, vol. 16, no. 4, pp. 678–688, 2001.

- [79] M. Herceg, M. Kvasnica, C. N. Jones, and M. Morari, “Multi-parametric toolbox 3.0,” *European Control Conference (ECC)*, pp. 502–510, 2013.
- [80] F. Borrelli, A. Bemporad, and M. Morari, *Predictive control for linear and hybrid systems*. Cambridge University Press, 2017.
- [81] A. Kurzhanskiĭ and I. Vályi, *Ellipsoidal calculus for estimation and control*. Nelson Thornes, 1997.
- [82] Z. Lin, B. Francis, and M. Maggiore, “Necessary and sufficient graphical conditions for formation control of unicycles,” *IEEE Transactions on Automatic Control*, vol. 50, no. 1, pp. 121–127, 2005.
- [83] G. Franzè and W. Lucia, “The obstacle avoidance motion planning problem for autonomous vehicles: A low-demanding receding horizon control scheme,” *Systems & Control Letters*, vol. 77, pp. 1–10, 2015.